NOSC

NOSC TR 535

LEVEL II

NOSC TR 535

Technical Report 535

THE DETECTABILITY OF A MINE USING REPLICA CORRELATION (RC) AND ECHO-ECHO CORRELATION (EEC)

MD Green

April 1980

Approved for public release; distribution unlimited.

NAVAL OCEAN SYSTEMS CENTER
SAN DIEGO, CALIFORNIA 92152

NAVAL OCEAN SYSTEMS CENTER, SAN DIEGO, CA 92152

AN ACTIVITY OF THE NAVAL MATERIAL COMMAND

SL GUILLE, CAPT, USN
Commander

HL BLOOD
Technical Director

ADMINISTRATIVE INFORMATION

The work reported herein was conducted over the period December 1979 to March 1980 in support of CNO Project SO239-AS, directed by NAVSEA Code 63X1.

The author wishes to express his appreciation to Mr. S. P. Pitt and Mr. J. Brady of ARL/UT for their help and suggestions.

Released by
RA McLennan, Head
Sonar Systems Division

Under authority of
RD Thuleen, Head
Weapon Control and Sonar Department

UNCLASSIFIED

SECURITY CLASSIFICATION OF THIS PAGE (When Data Entered)

REPORT DOCUMENTATION PAGE

READ INSTRUCTIONS BEFORE COMPLETING FORM

1. REPORT NUMBER: NOSC Technical Report 535 (TR 535)	2. GOVT ACCESSION NO.: AD-A086 825
3. RECIPIENT'S CATALOG NUMBER	
4. TITLE (and Subtitle): The Detectability of a Mine Using Replica Correlation (RC) and Echo-Echo Correlation (EEC)	5. TYPE OF REPORT & PERIOD COVERED: Research report Dec 1979–March 1980
	6. PERFORMING ORG. REPORT NUMBER
7. AUTHOR(s): M. D. Green	8. CONTRACT OR GRANT NUMBER(s)
9. PERFORMING ORGANIZATION NAME AND ADDRESS: Naval Ocean Systems Center, San Diego, CA 92152	10. PROGRAM ELEMENT, PROJECT, TASK AREA & WORK UNIT NUMBERS: S0239-AS; PS0239A15
11. CONTROLLING OFFICE NAME AND ADDRESS: Chief of Naval Operations, Washington, DC 20350	12. REPORT DATE: April 1980
	13. NUMBER OF PAGES: 42
14. MONITORING AGENCY NAME & ADDRESS (if different from Controlling Office)	15. SECURITY CLASS. (of this report): Unclassified
	15a. DECLASSIFICATION/DOWNGRADING SCHEDULE

16. DISTRIBUTION STATEMENT (of this Report)

Approved for public release; distribution unlimited. NOSC/TR-535

17. DISTRIBUTION STATEMENT (of the abstract entered in Block 20, if different from Report)

18. SUPPLEMENTARY NOTES

19. KEY WORDS (Continue on reverse side if necessary and identify by block number)

20. ABSTRACT (Continue on reverse side if necessary and identify by block number)

The detectability of a small target by means of active sonar must be discussed in terms of waveform characteristics and the signal processing used to extract the echo from interference. This report presents the target signature of a mine for large bandwidth-time product (BT) waveforms, and discusses the losses suffered when the echo is processed by Replica Correlation (RC) and Echo-Echo Correlation (EEC). It is shown that RC "splitting" losses increase with bandwidth, while EEC losses are relatively independent of bandwidth and are much lower than RC losses. The detectability of this mine for a given scenario of false alarm rate, number of beams, sonar platform motion, and processing type is also included.

DD FORM 1 JAN 73 1473 EDITION OF 1 NOV 65 IS OBSOLETE S/N 0102-LF-014-6601

UNCLASSIFIED

SECURITY CLASSIFICATION OF THIS PAGE (When Data Entered)

393 159

CONTENTS

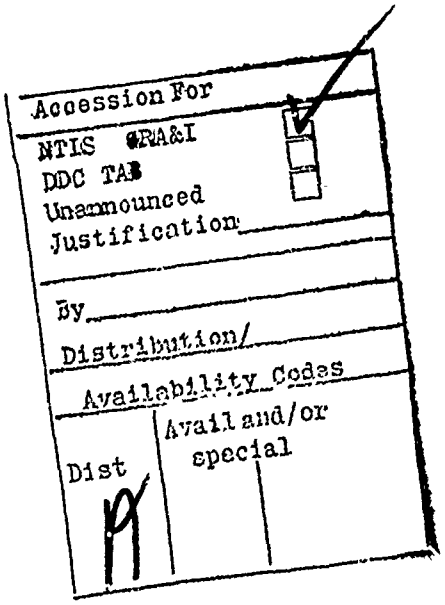

I. INTRODUCTION

This paper is concerned with the acoustic detection of underwater mines from the standpoint of signal characteristics and signal processing. The work that has been done in the field has relied primarily on target response to CW pulses, with the echo processed by a simple rectifier and averager (Refs. 1, 2). With modern microprocessors, it is now feasible to employ more complex signals such as linear frequency modulated (LFM) pulses and pseudo-random noise (PRN) pulses that offer greater Doppler tolerance, better noise rejection, and much greater signal energy than is possible with short CW. The use of such signals, however, presents its own problems, particularly as regards ocean multipath and target structural response to the incident acoustic energy. Since adequate data were not available concerning the response of actual mines to these types of pulses, it was decided to conduct an experiment to determine the response of a particular mine (Ref. 3) to several representative waveforms. The test was devised and conducted as a joint project between the Applied Research Laboratory (ARL) at the University of Texas, and the Naval Ocean Systems Center (NOSC), San Diego, California.

One of the measures customarily required by the sonar engineer is the reflectivity index of a target generally referred to as the "target strength." Practically, this would be a ratio of the received echo power to the transmitted power, once interfering effects such as propagation loss and absorption are accounted for. One problem that arises, the one pertinent to this discussion, is the difficulty in making quantitative measurements of the received echo. As shown later, the echo structure is highly dependent on the aspect angle of the target, and as such, would be very difficult to measure in an operational environment.

The detectability of an acoustic target when using relatively complex waveforms is enhanced by some form of signal processing. Two types of coherent processing are discussed in this paper, namely Replica Correlation (RC) (Refs. 4, 5) and Echo-Echo Correlation (EEC) (Ref. 5), in terms of their ability to increase the detectability of this mine.

II. TEST PROCEDURE

The Target Strength Measurement Facility at ARL (Ref. 6) was used to conduct this experiment. The target was held as shown in figure 1, with the major axis in the horizontal plane of the hydrophones. The control mechanism allows either continuous rotation of the body, or rotation to fixed aspect angles, as desired. For this experiment the target was rotated to twenty different, discrete aspect angles. The target geometry is shown in figure 2, with the aspect angles investigated listed on that figure. Note that the "zero" aspect angle for this target occurs at broadside, a peculiarity of the ARL rotator.

The transmit pulses were generated by a programmable device designed at ARL. The eight pulse codes (PC's) used are listed in table 1. At the conclusion of the eightieth transmission, the target was moved to the next aspect angle, and the sequence repeated.

PC	B(kHz)	T(ms)	Type
1	1	100	LFM single
2	2	100	LFM single
3	4	100	LFM single
4	1	3X24.6	LFM triplet
5	2	3X24.6	LFM triplet
6	4	3X24.6	LFM triplet
7	4	100	PRN single
8	4	3X24.6	PRN triplet

B = bandwidth, T = pulse length; Center Frequency = 27.6kHz

Table 1. Experimental waveforms.

In addition to the target, a calibrated probe was placed at a known distance from the hydrophone for one series of transmissions. The data obtained were intended for measuring path loss and target strength and system distortion.

The acoustic returns were electronically gated so that a small portion of pre-echo noise, the echo, and some trailing noise were recorded. The gated returns were sampled with a 12-bit digitizer and the samples stored on magnetic tape.

Finally, a series of pulses was sampled directly at the output of the signal generator, and the samples were stored as before for use as replicas in later signal processing.

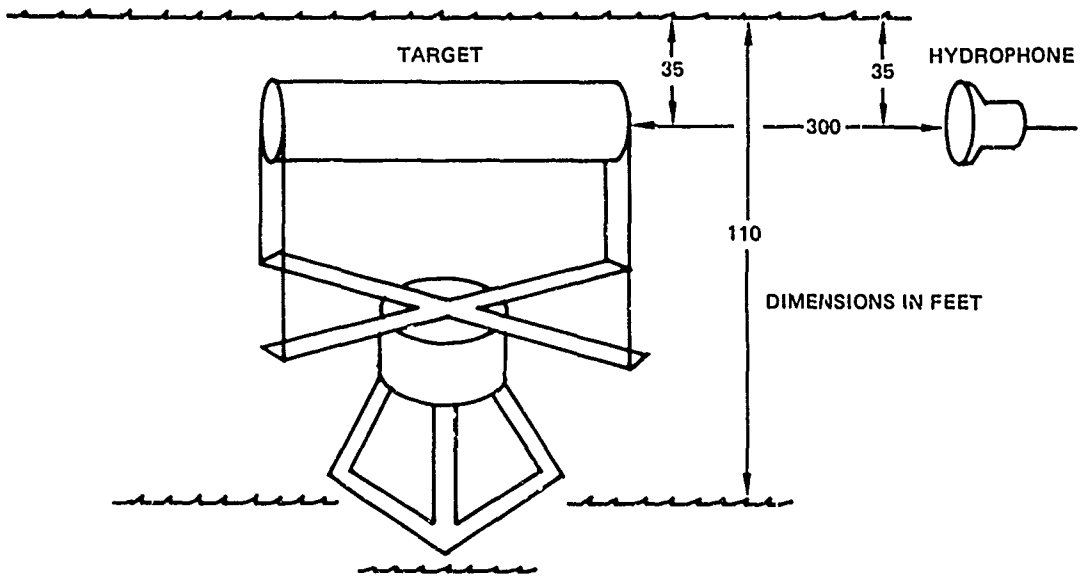

Figure 1. Target rotator.

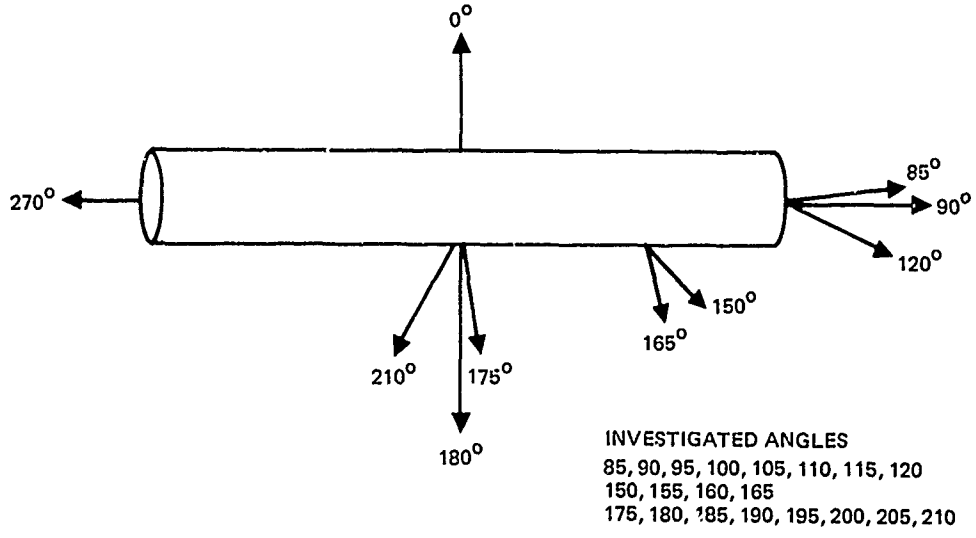

Figure 2. Target geometry.

III. SIGNAL PROCESSING AND DATA REDUCTION

The pulses discussed in this paper all have bandwidth – time products (BT) much greater than a CW pulse. The use of these pulses in acoustic detection is enhanced by some form of processing which reduces the BT product to a lower value. This may be accomplished by incoherent processing, such as rectification followed by averaging or by coherent processing, such as correlation. The latter approach is considered here, and is limited to Replica Correlation and Echo-Echo Correlation. RC is the "optimum" filter for an echo imbedded in Gaussian, white noise, when that echo exactly replicates the transmitted pulse, while EEC is a relatively new process which tends to account for environmental and target induced distortions of the echo. A summary of the EEC process is given in the appendix. In the RC case, for an ideal situation of echo perfectly matched to the transmitted pulse, the peak of the correlation of the echo should represent the acoustic power contained in the echo. For EEC, an equivalent result should hold, regardless of the mismatch between transmit pulse and echo.

The data reduction falls into three categories. First, ten echoes for each pulse code at each aspect angle were envelope detected, squared, and averaged together. The results are shown in figures 3-10. The average power at each aspect angle was determined as the average mean square amplitude of the echo set prior to detection. Second, each echo was correlated with its appropriate replica. The resulting curves were envelope detected, squared, and averaged together as was done for the echoes. The resulting curves are shown in figures 11-18. Note that the time axis has been expanded to show 30ms about the main peak. Third, the EEC process was performed for the appropriate echoes (PC 4, 5, 6, 8), the results envelope detected, squared, and averaged, as was done previously. The results are shown in figures 19-22. The plots present the same expansion of the peaks as do the RC plots, but the abscissa must be interpreted as discussed in the appendix. The vertical scale for the three sets of plots is indicated on each plot.

Finally, the processing gain available for the two types of correlation was explored. To that end, ten independent, Gaussian, bandlimited white noise populations, each normalized to an integrated power spectral density of unity, were added in succession to the successive echoes for the desired pulse codes, for selected aspect angles. The input signal to noise ratio was computed as

$$SNi = Power/\sigma_i^2 \tag{1}$$

where: "Power" is taken from the echo plots, figs 3-10 as appropriate; σ_i^2 is the average variance of the input noise populations (a multiplicative scale factor).

The output signal to noise ratios were computed as

$$SNo = Peak/\sigma_o^2 \tag{2}$$

where: "Peak" is the highest (average) output of signal plus noise; σ_o^2 is the average variance of the noise only correlation output, prior to envelope detection.

The theoretical SNo's (Ref. 5) are, for RC

$$SNo = 2BT(SNi), \tag{3}$$

and for EEC

$$SNo = 2BT(SNi)^2. \tag{4}$$

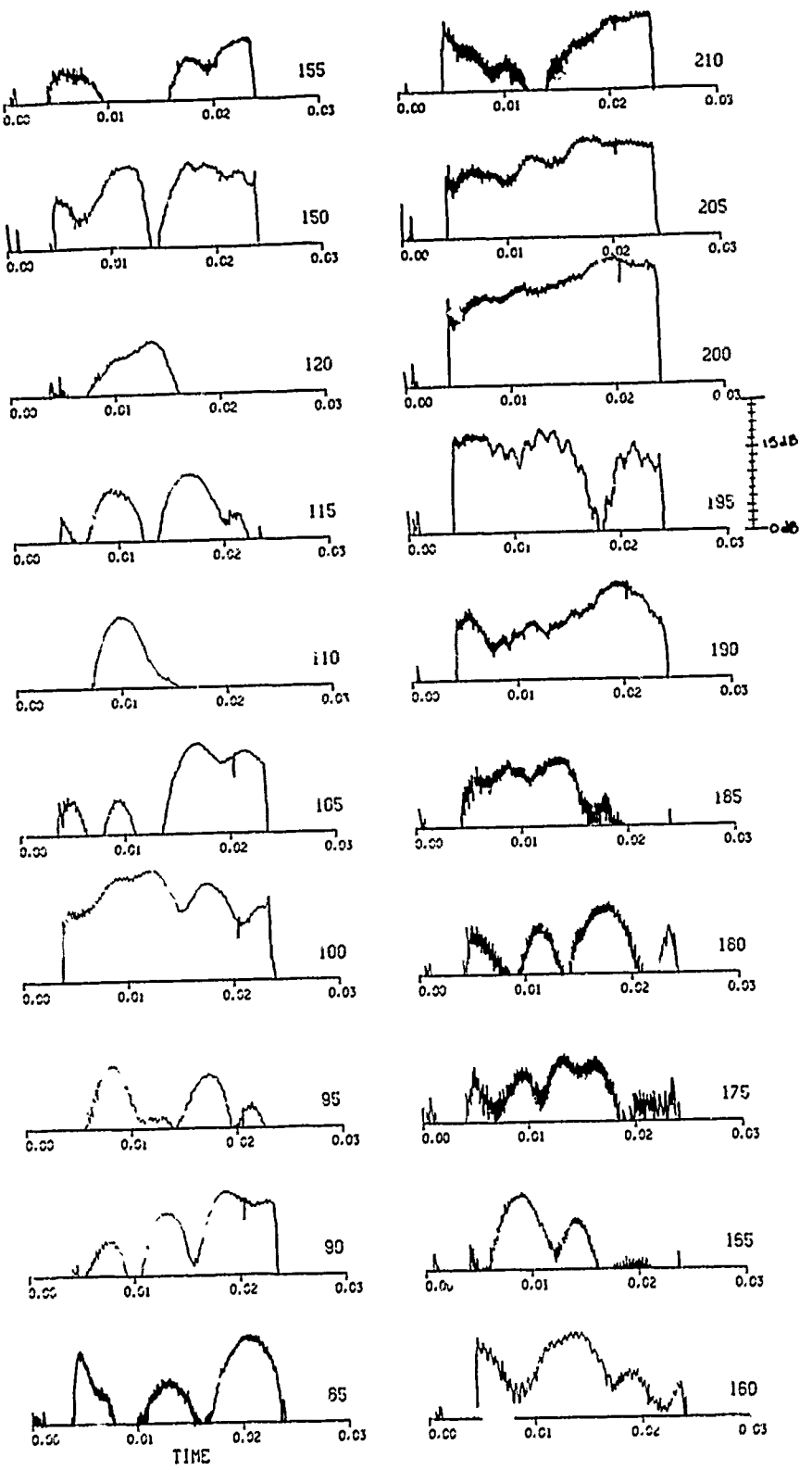

Figure 3. Pulse code 1.

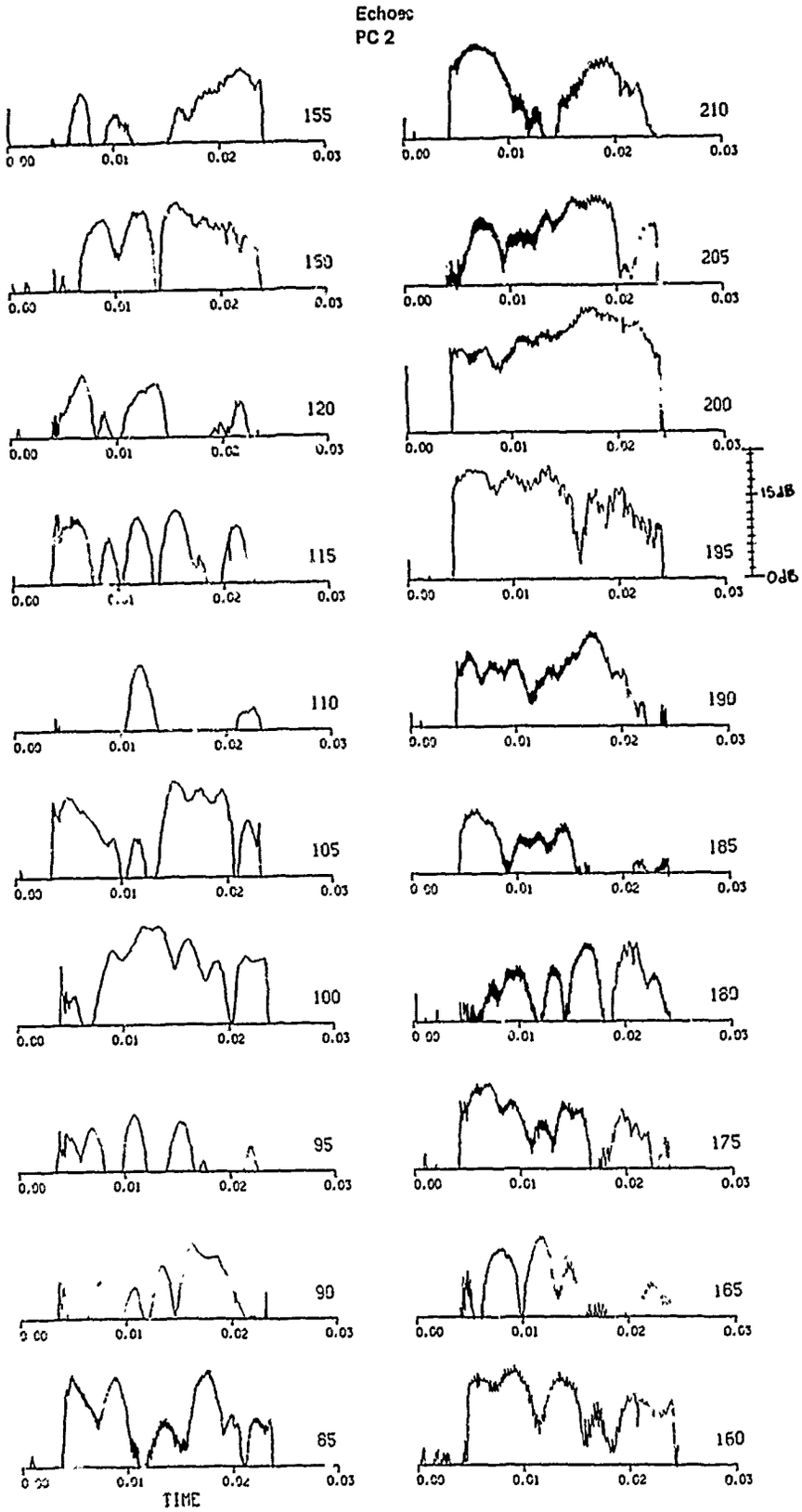

Figure 4. Pulse Code 2.

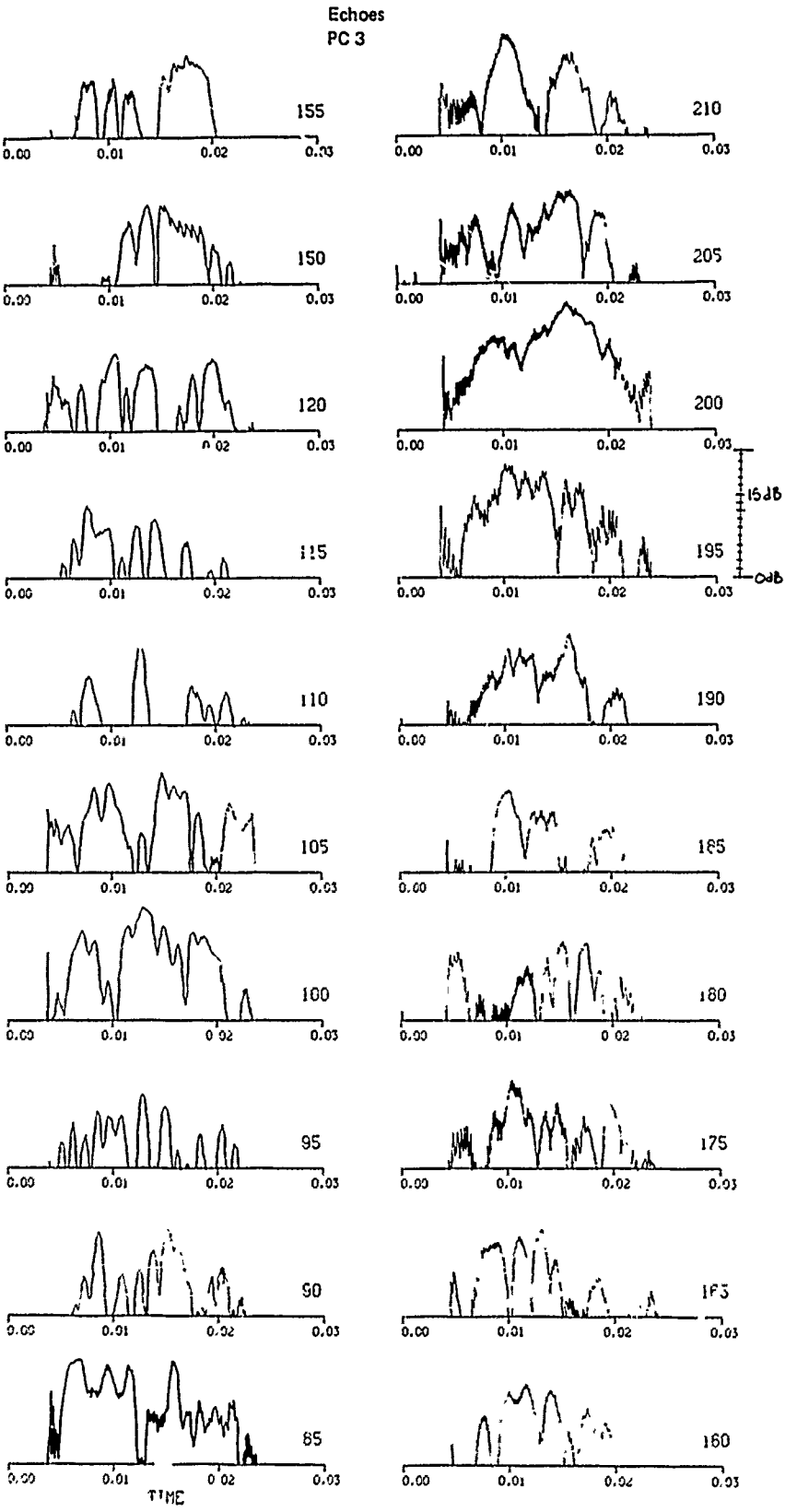

Figure 5. Pulse Code 3.

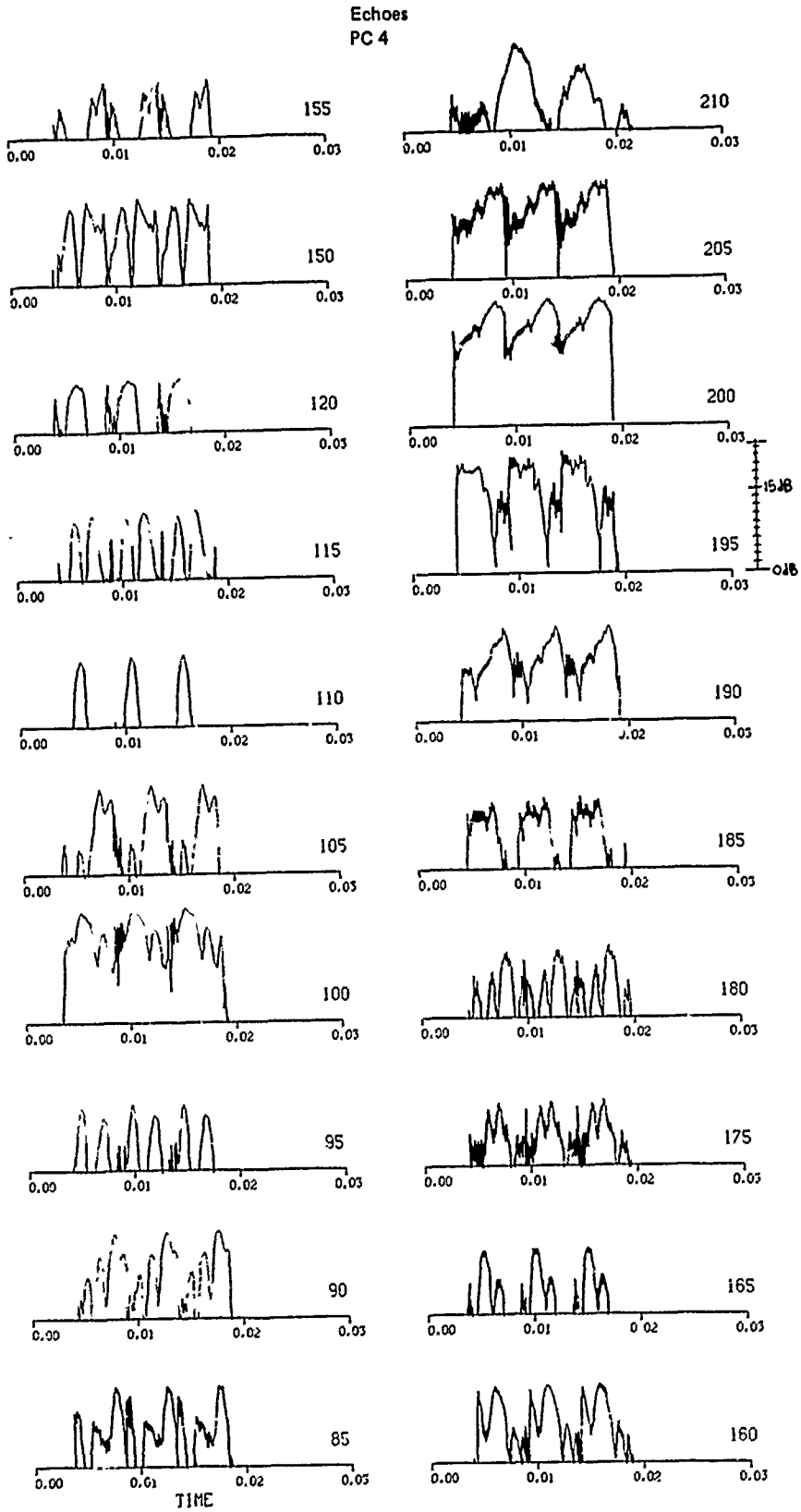

Figure 6. Pulse Code 4.

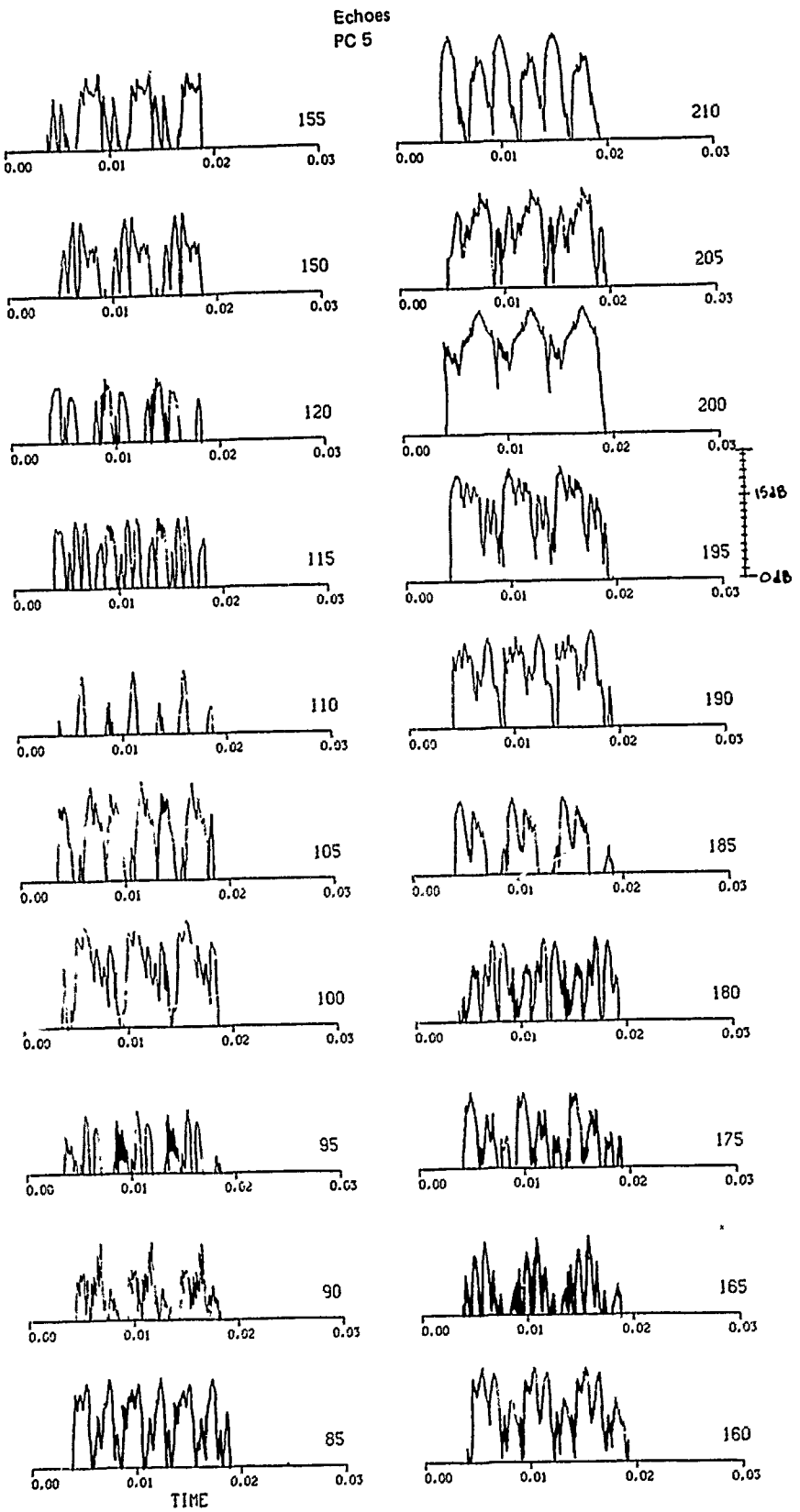

Figure 7. Pulse Code 5.

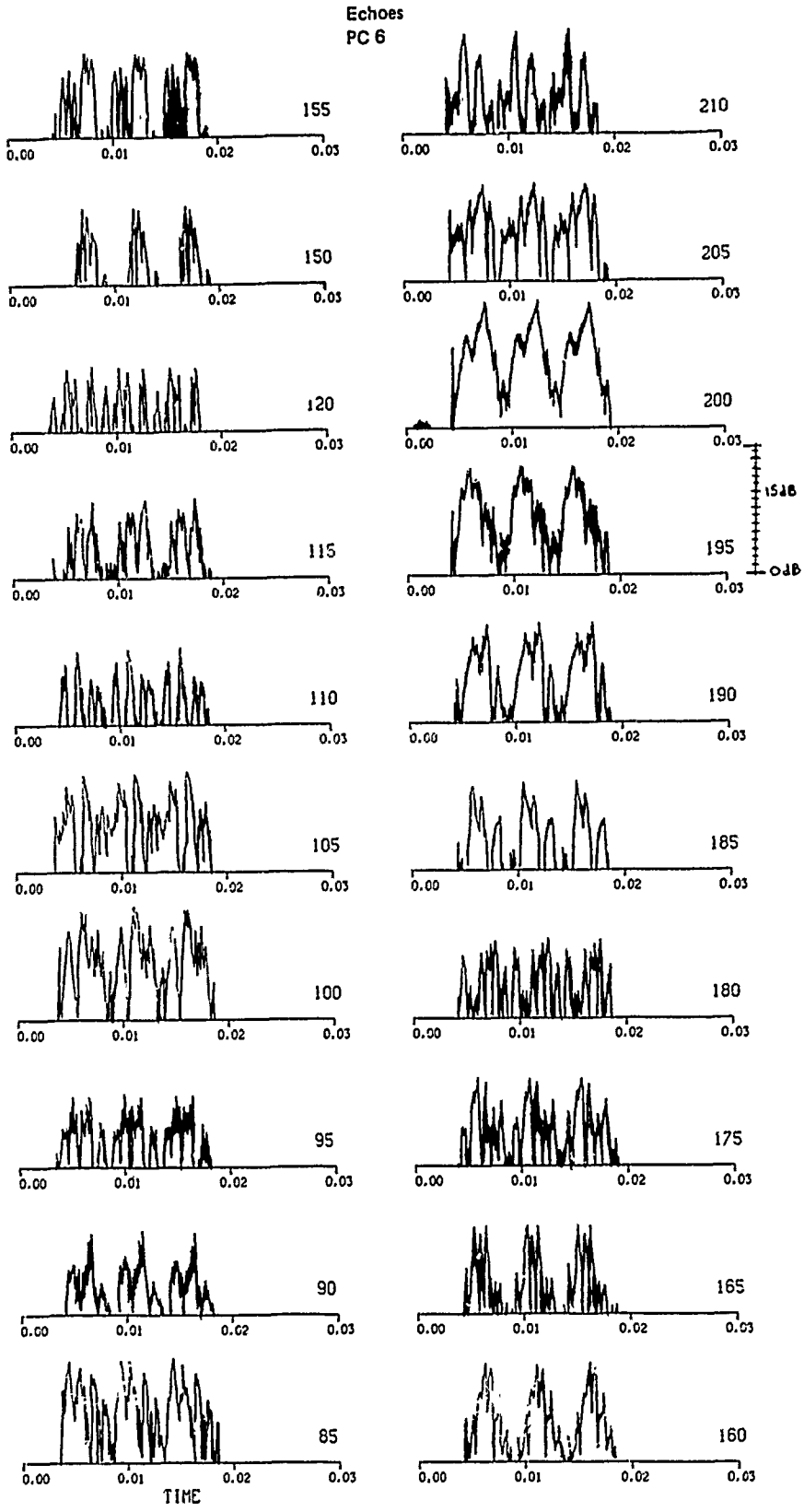

Figure 8. Pulse Code 6.

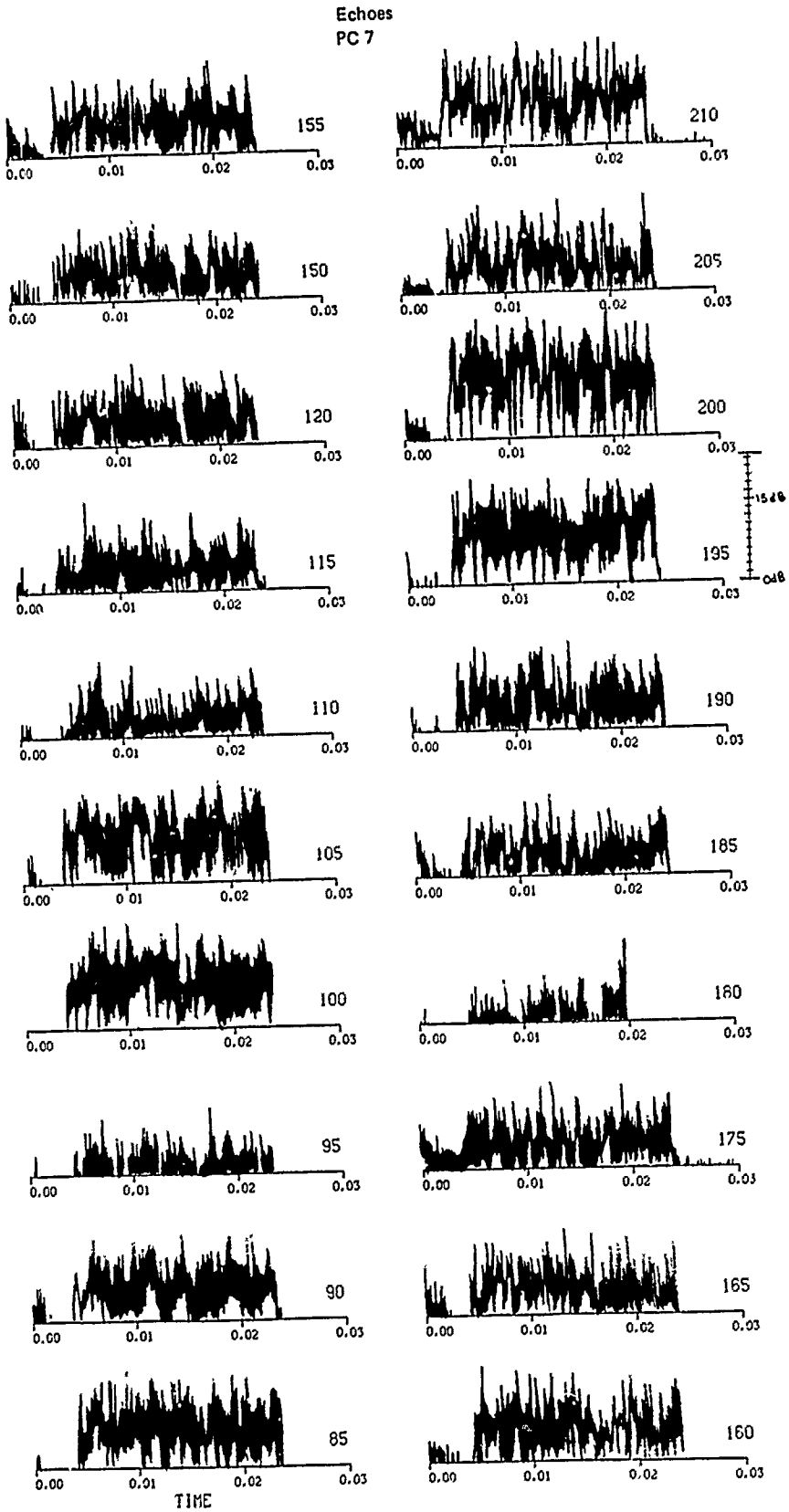

Figure 9. Pulse Code 7.

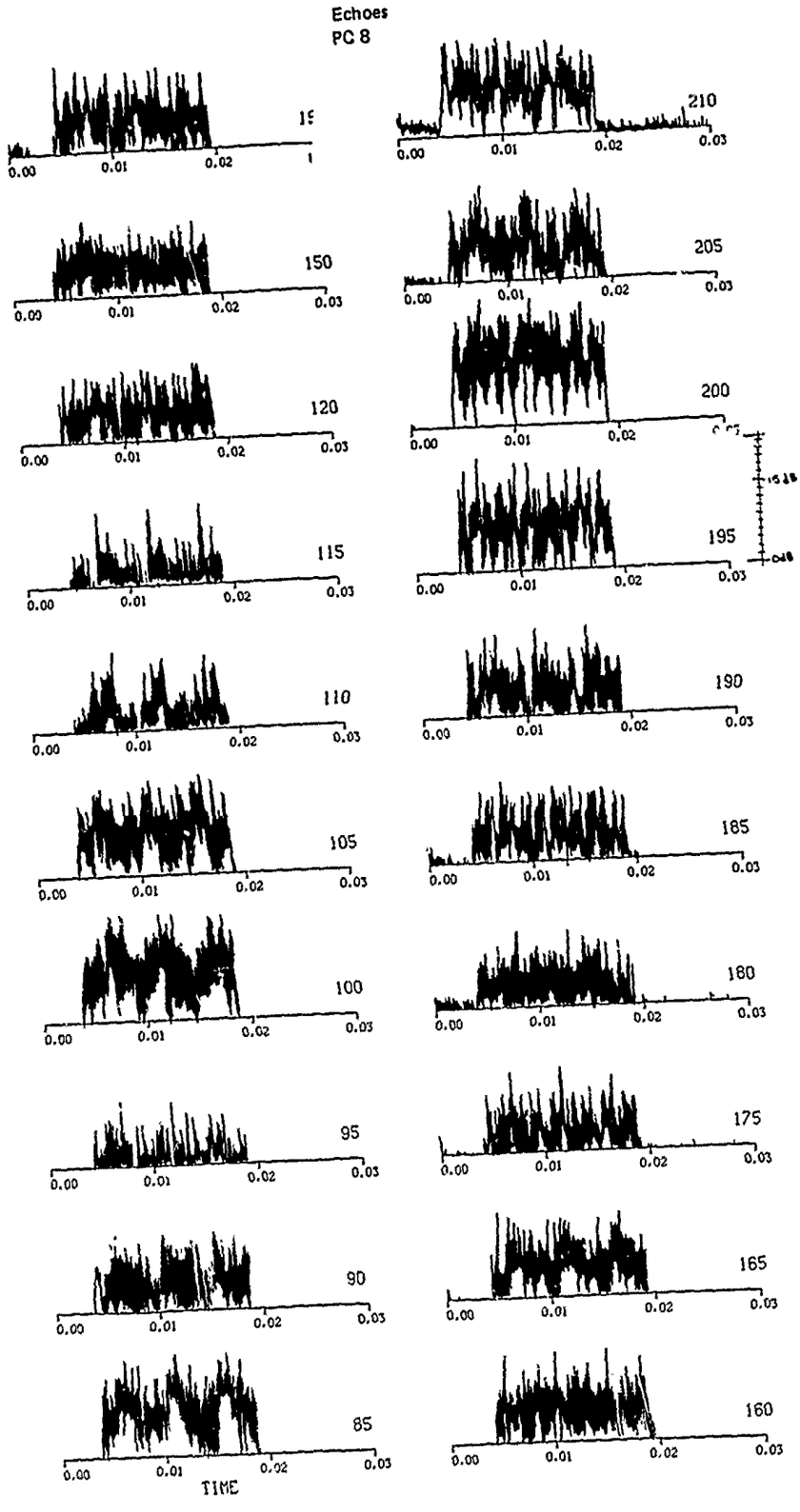

Figure 10. Pulse Code 8.

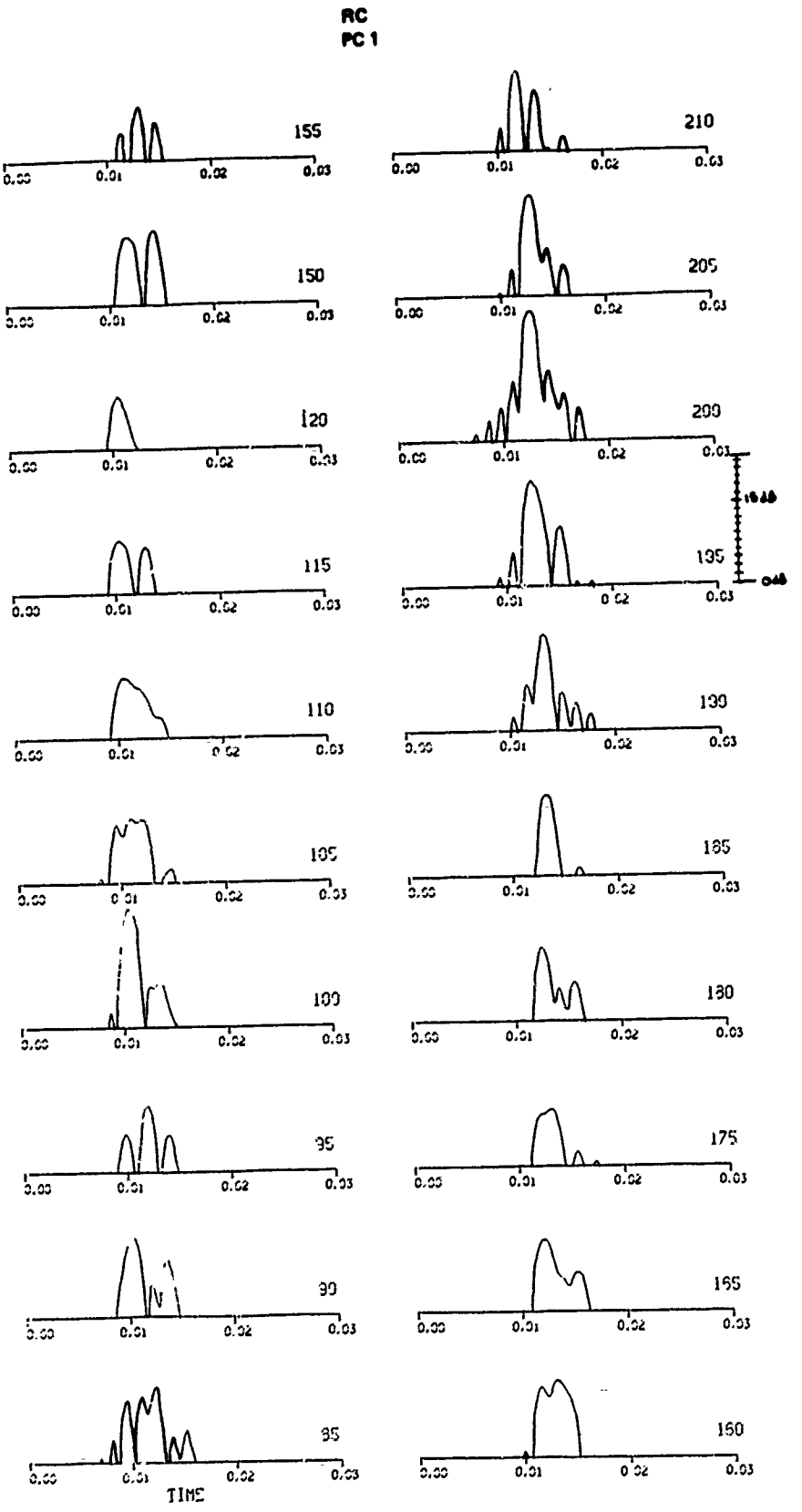

Figure 11. Pulse Code 1.

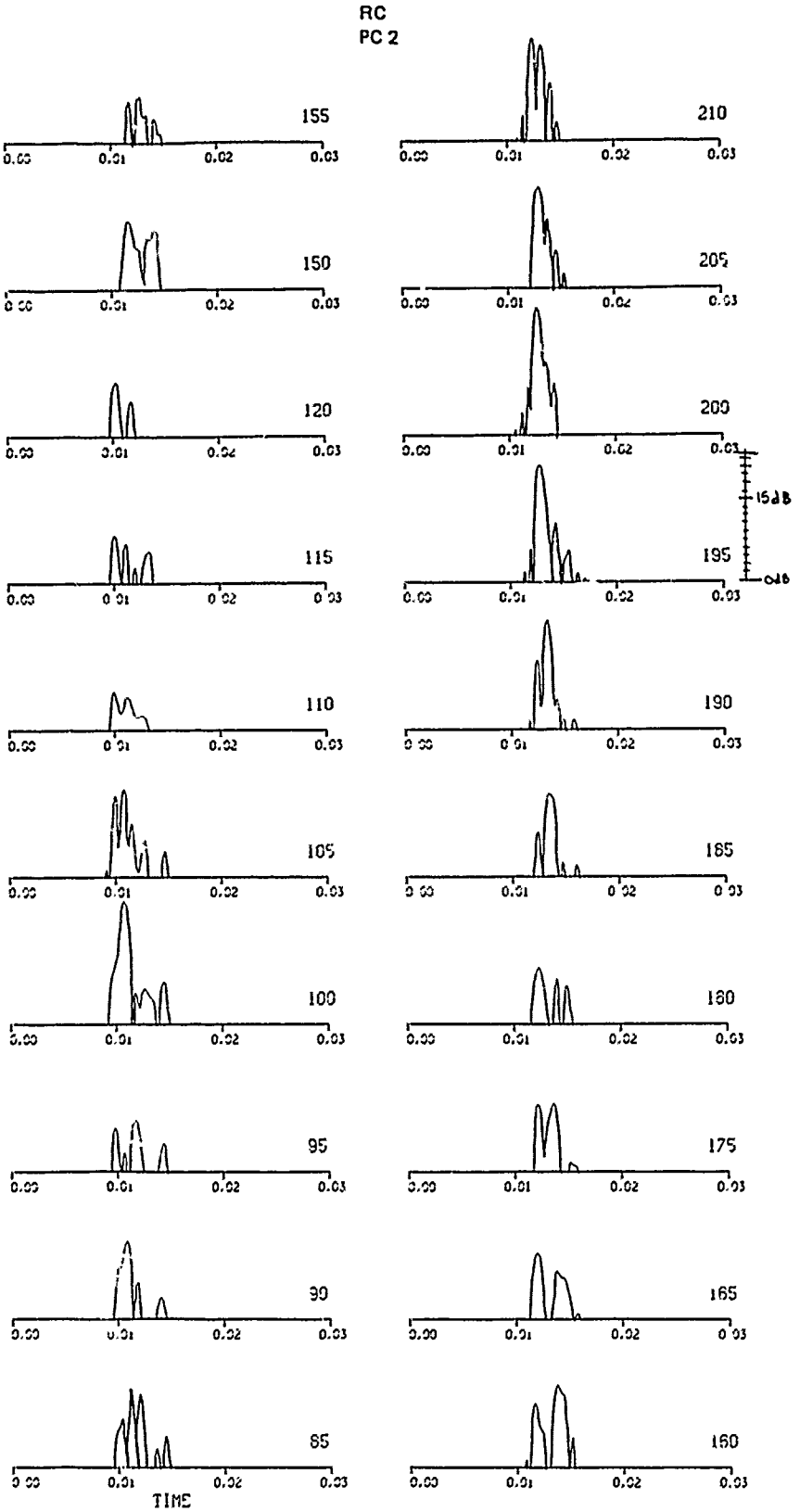

Figure 12. Pulse Code 2.

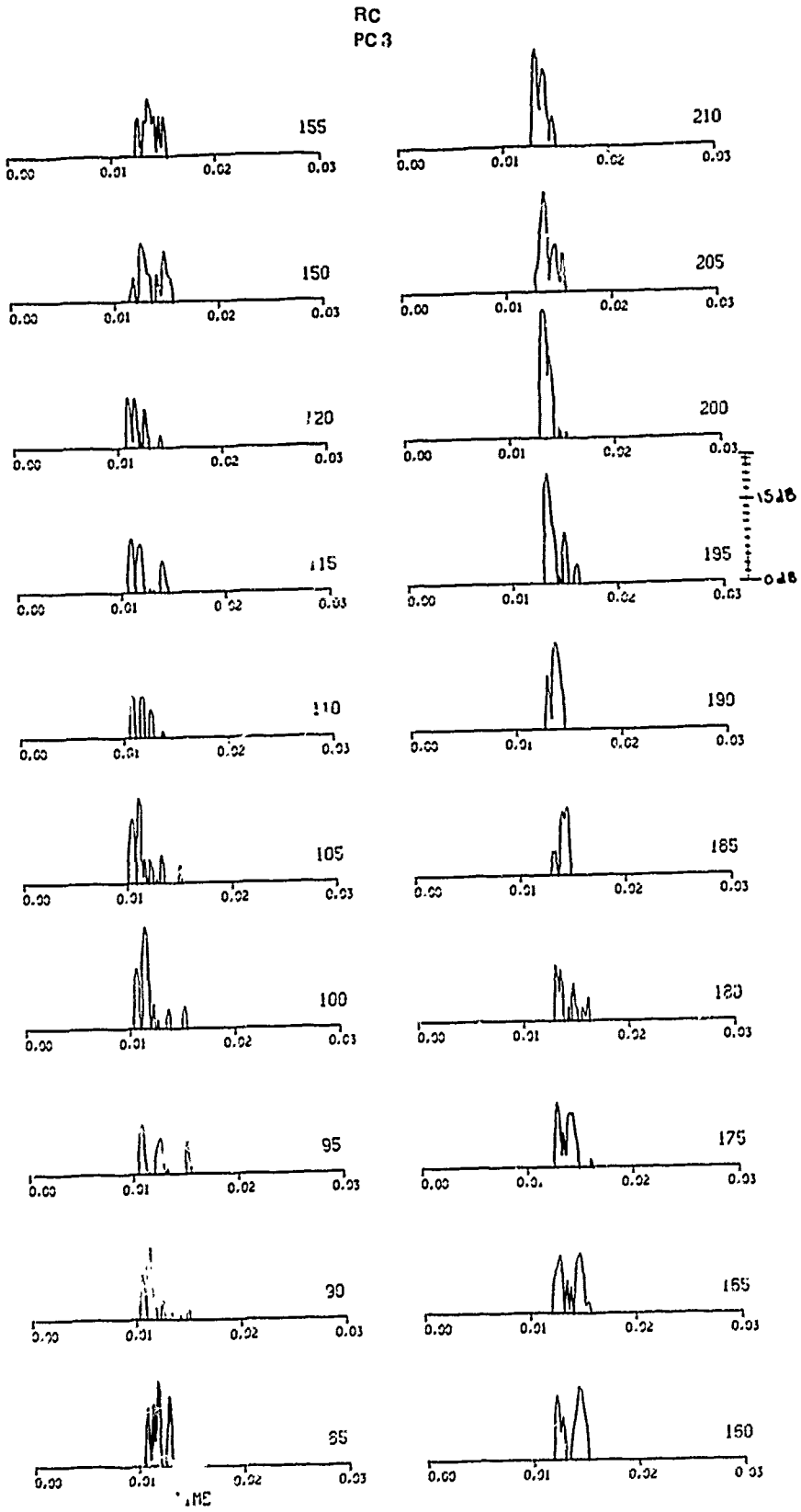

Figure 13. Pulse Code 3.

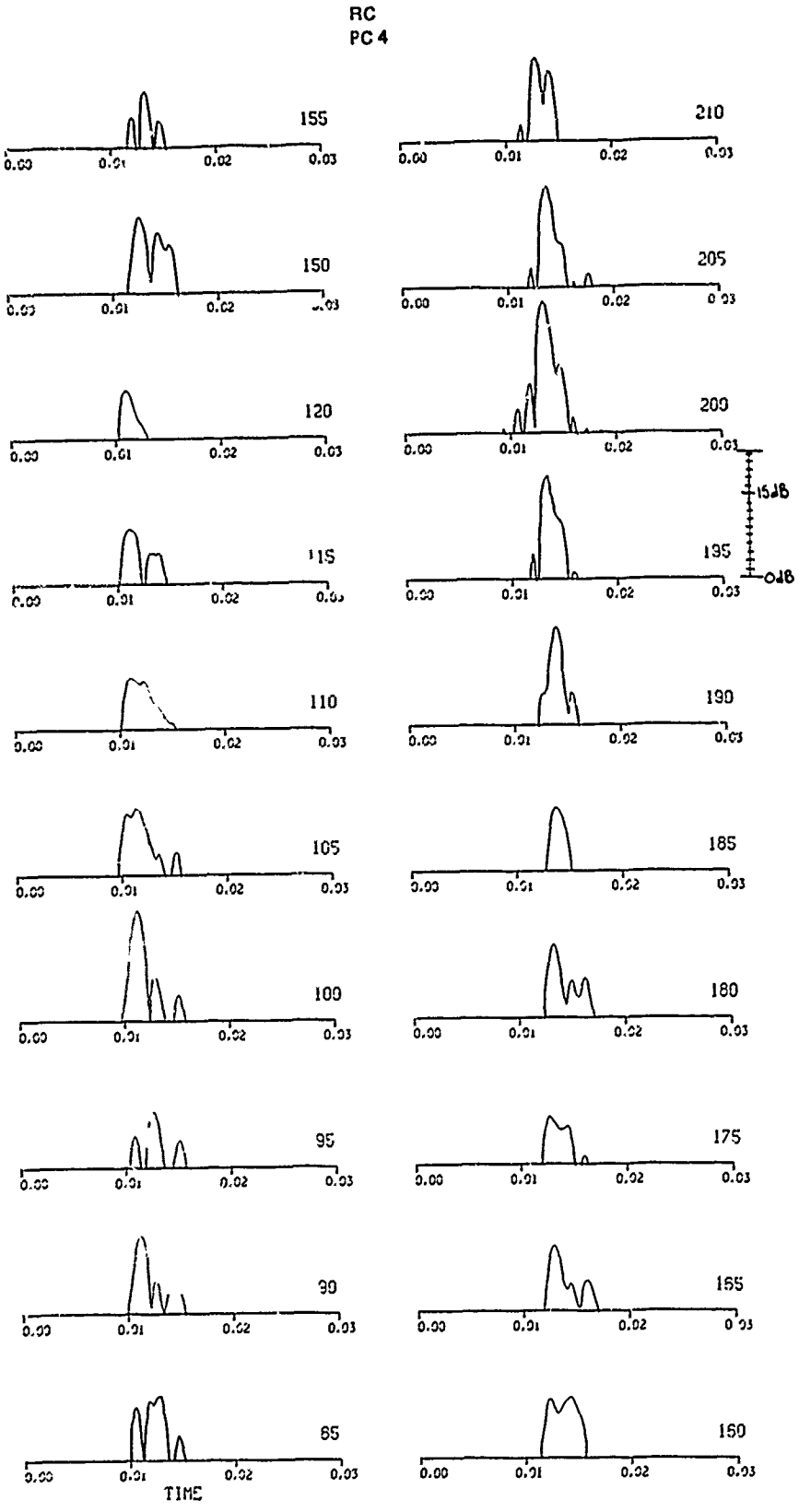

Figure 14. Pulse Code 4.

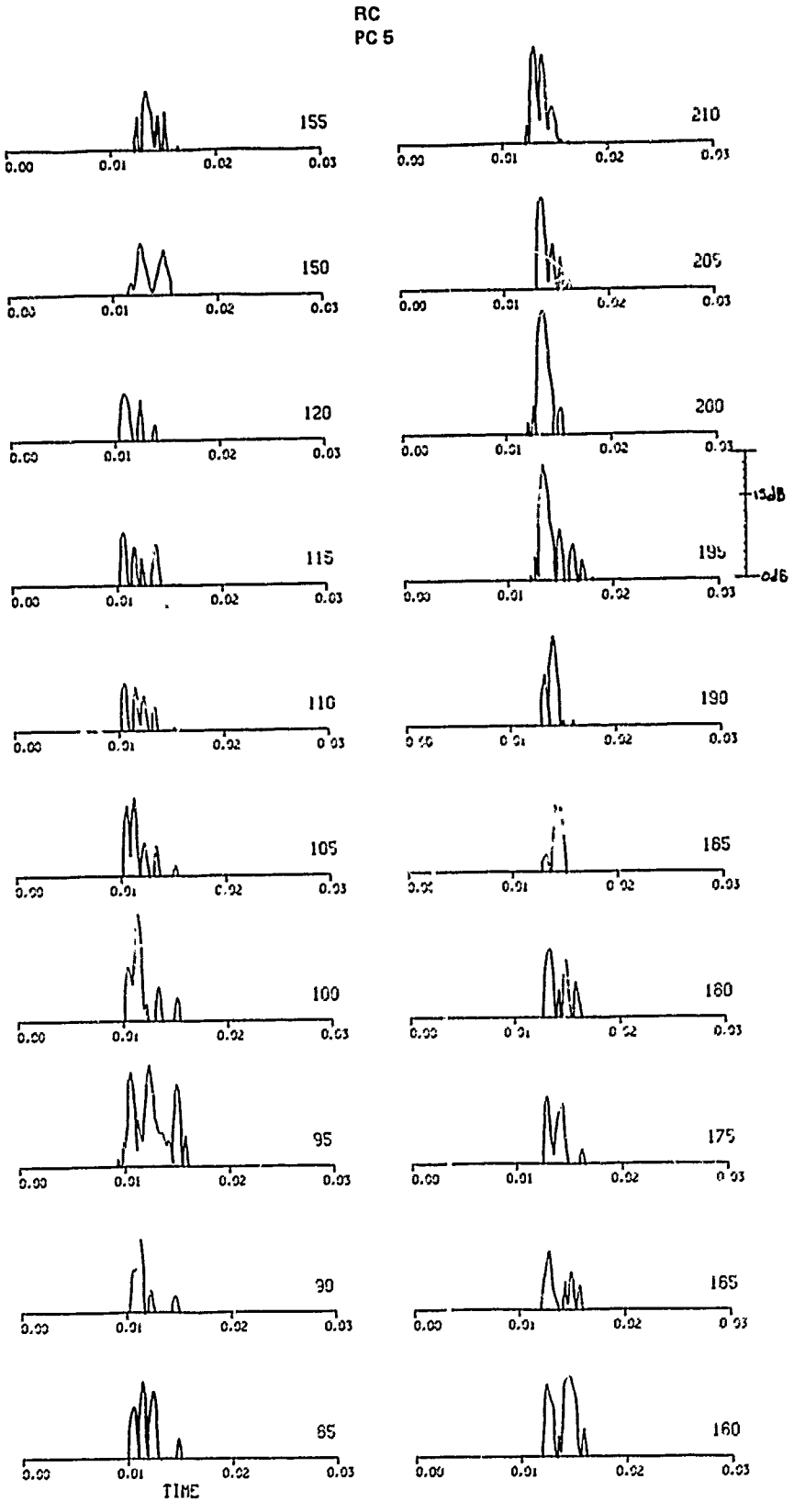

Figure 15. Pulse Code 5.

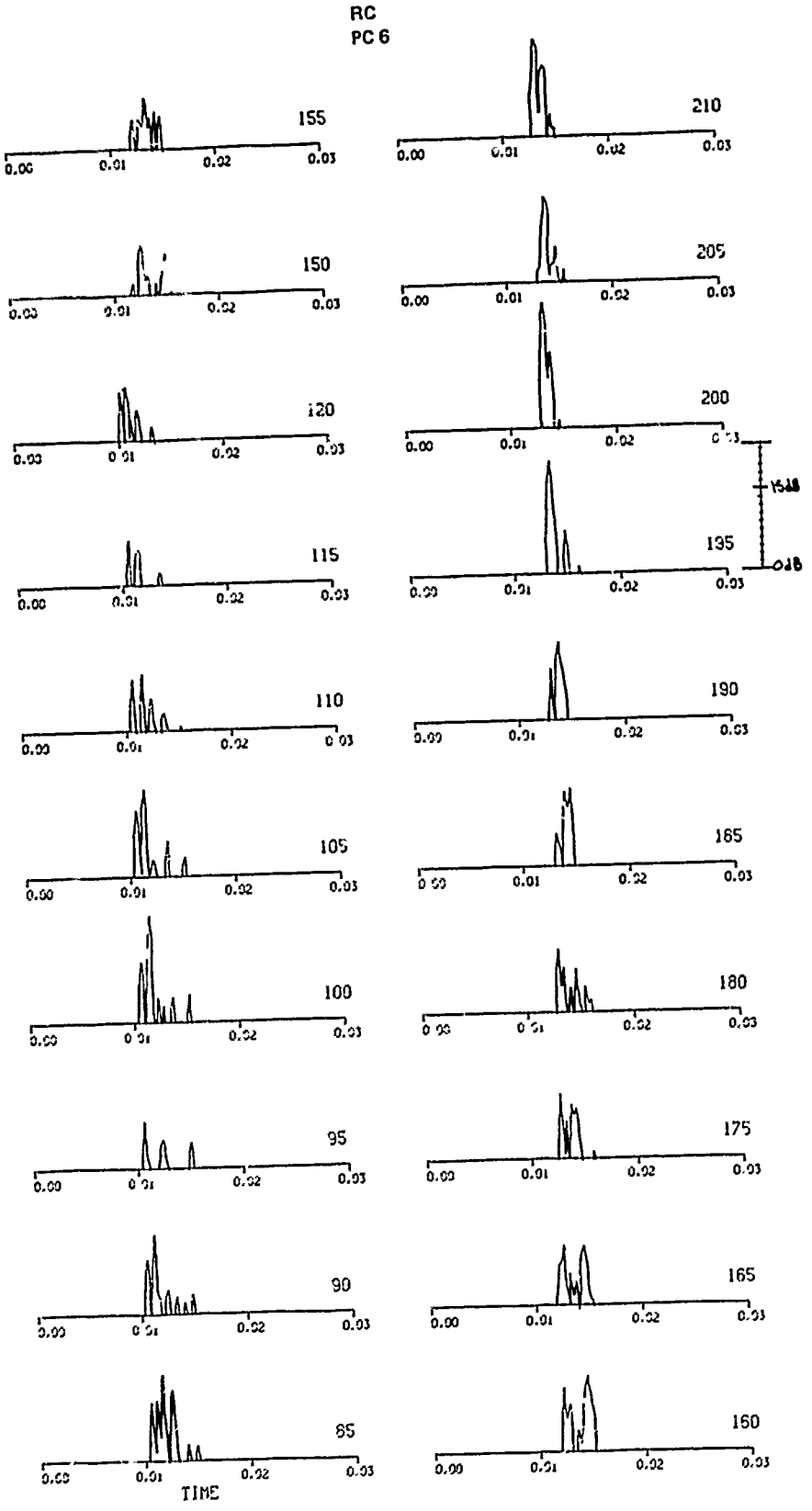

Figure 16. Pulse Code 6.

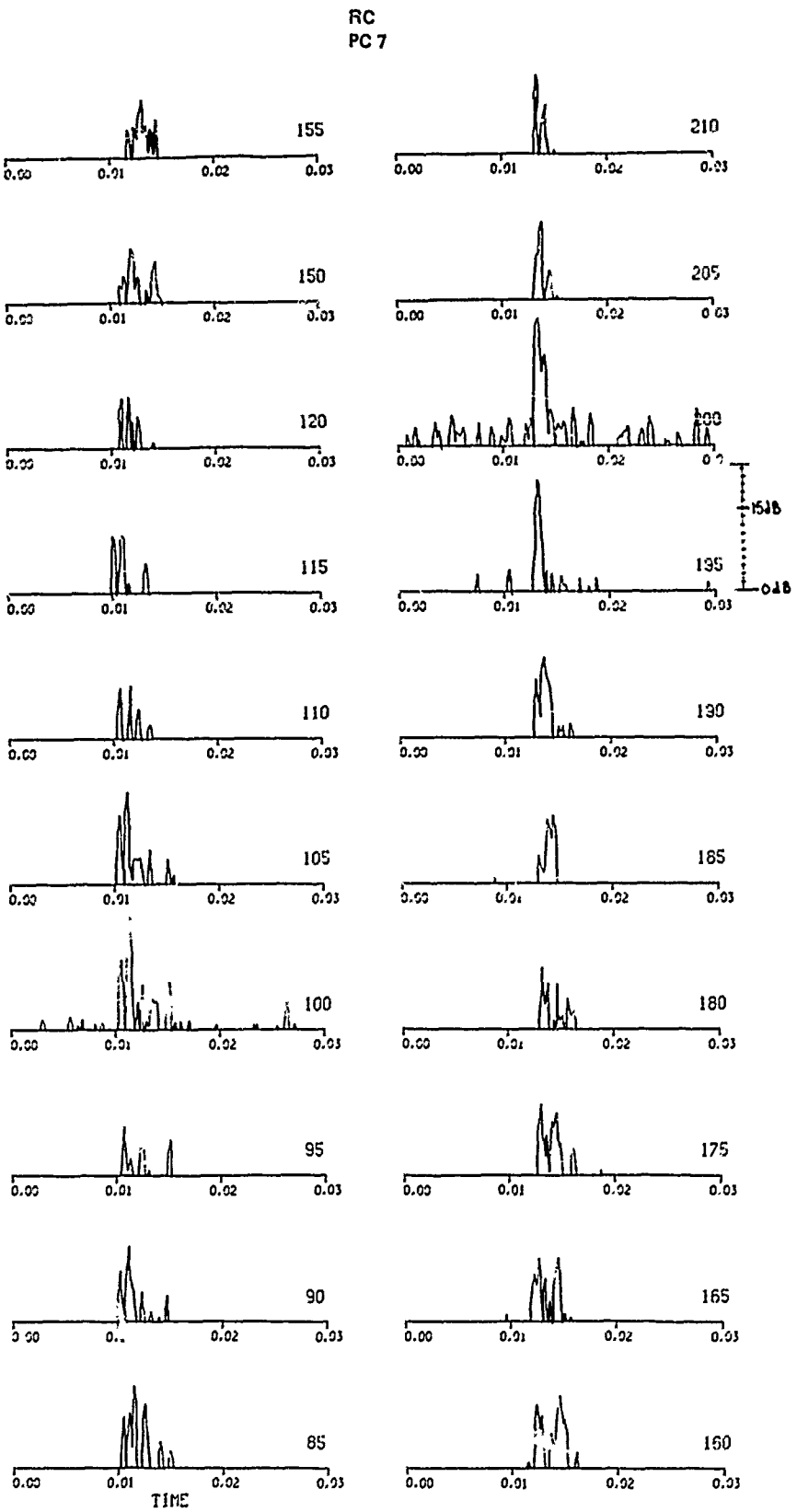

Figure 17. Pulse Code 7.

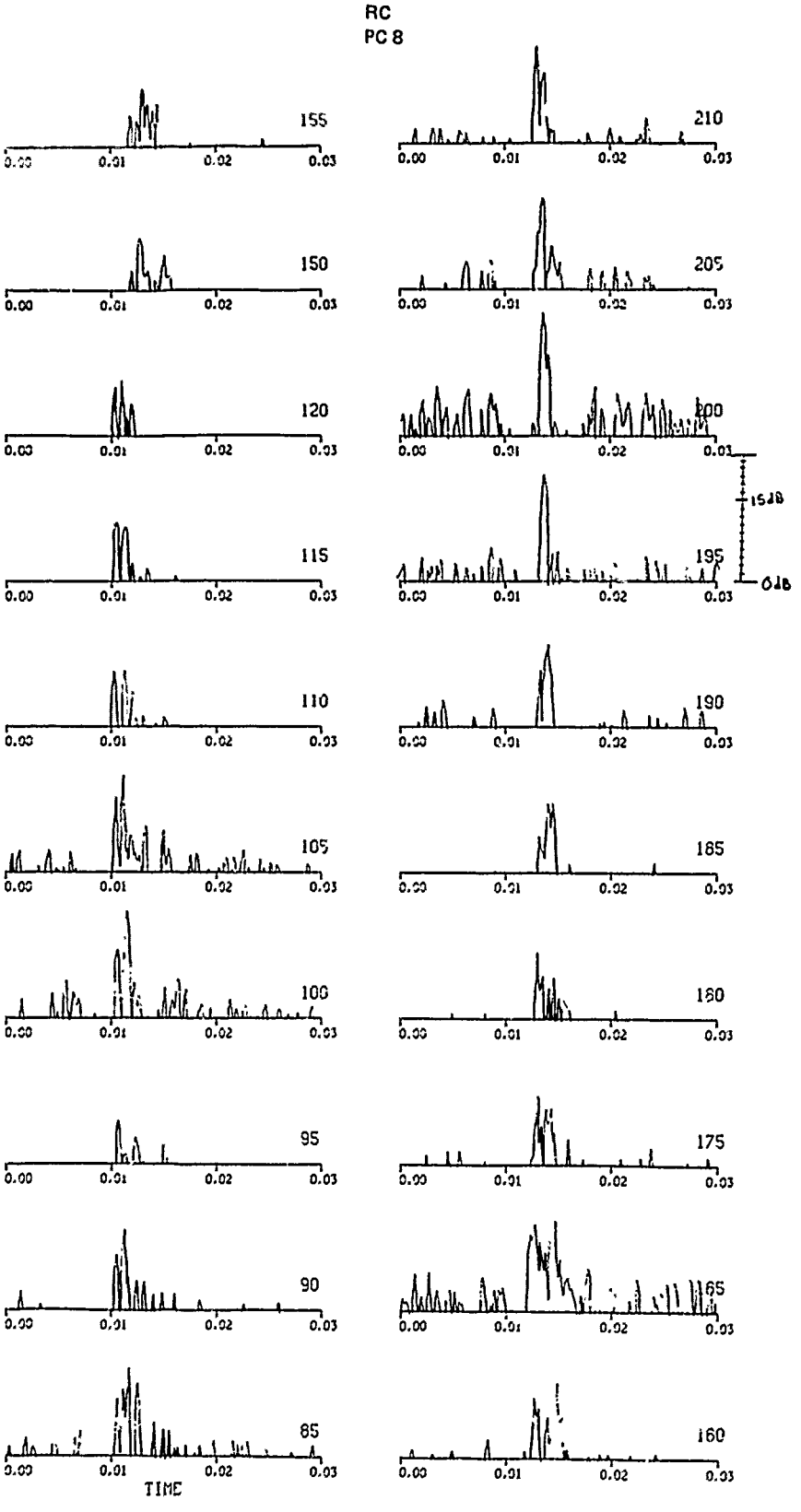

Figure 18. Pulse Code 8.

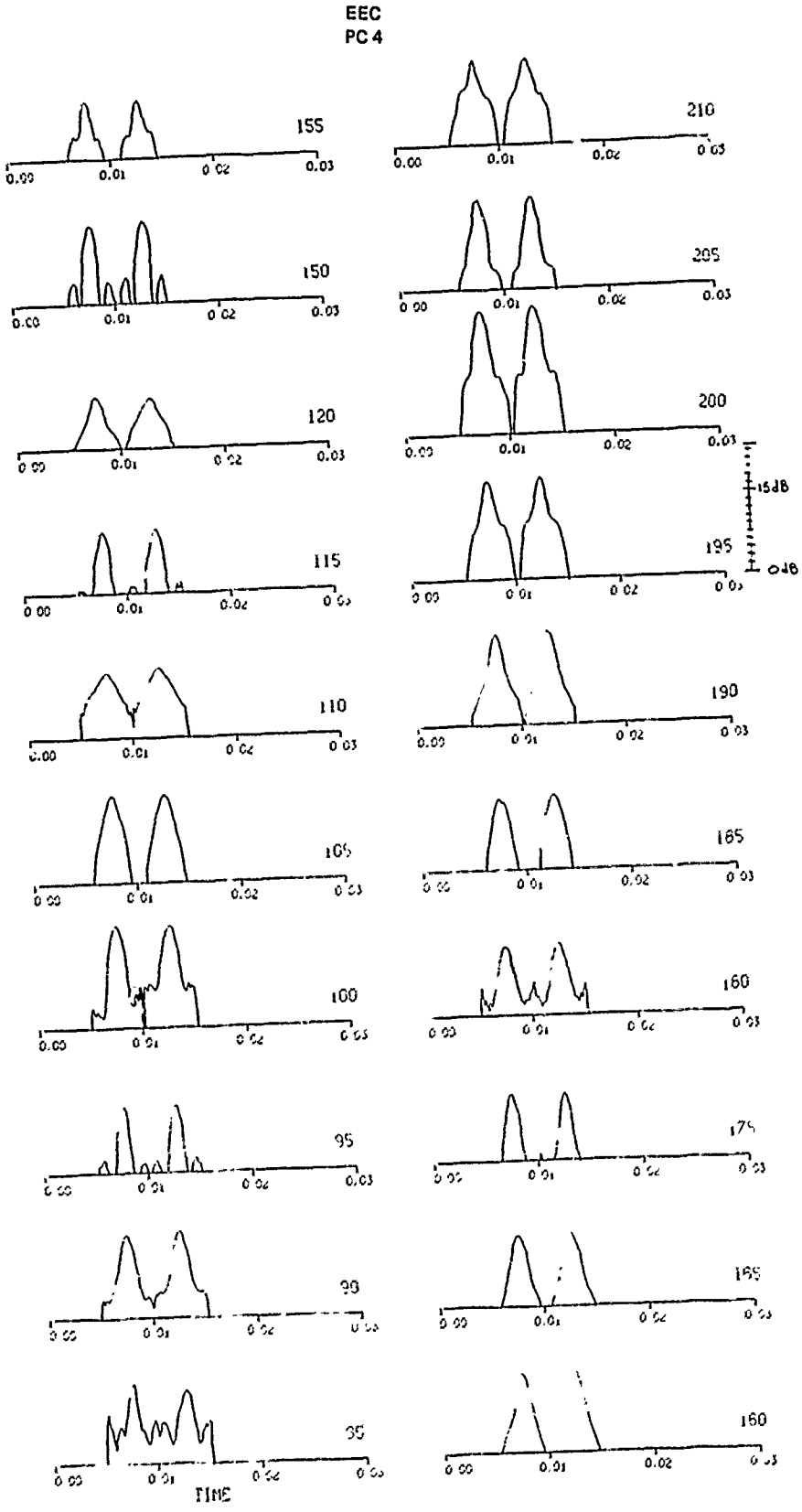

Figure 19. Pulse Code 4.

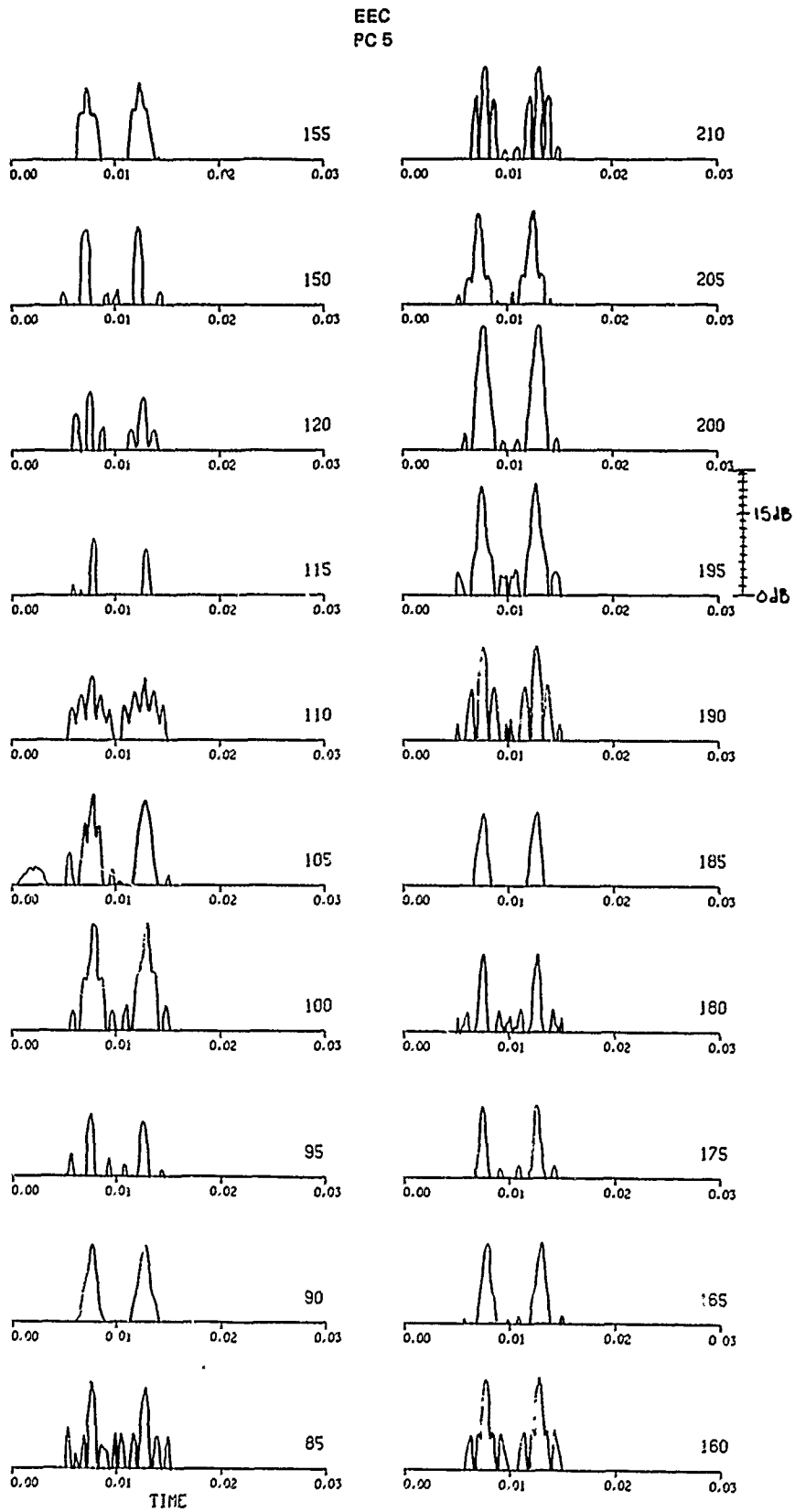

Figure 20. Pulse Code 5.

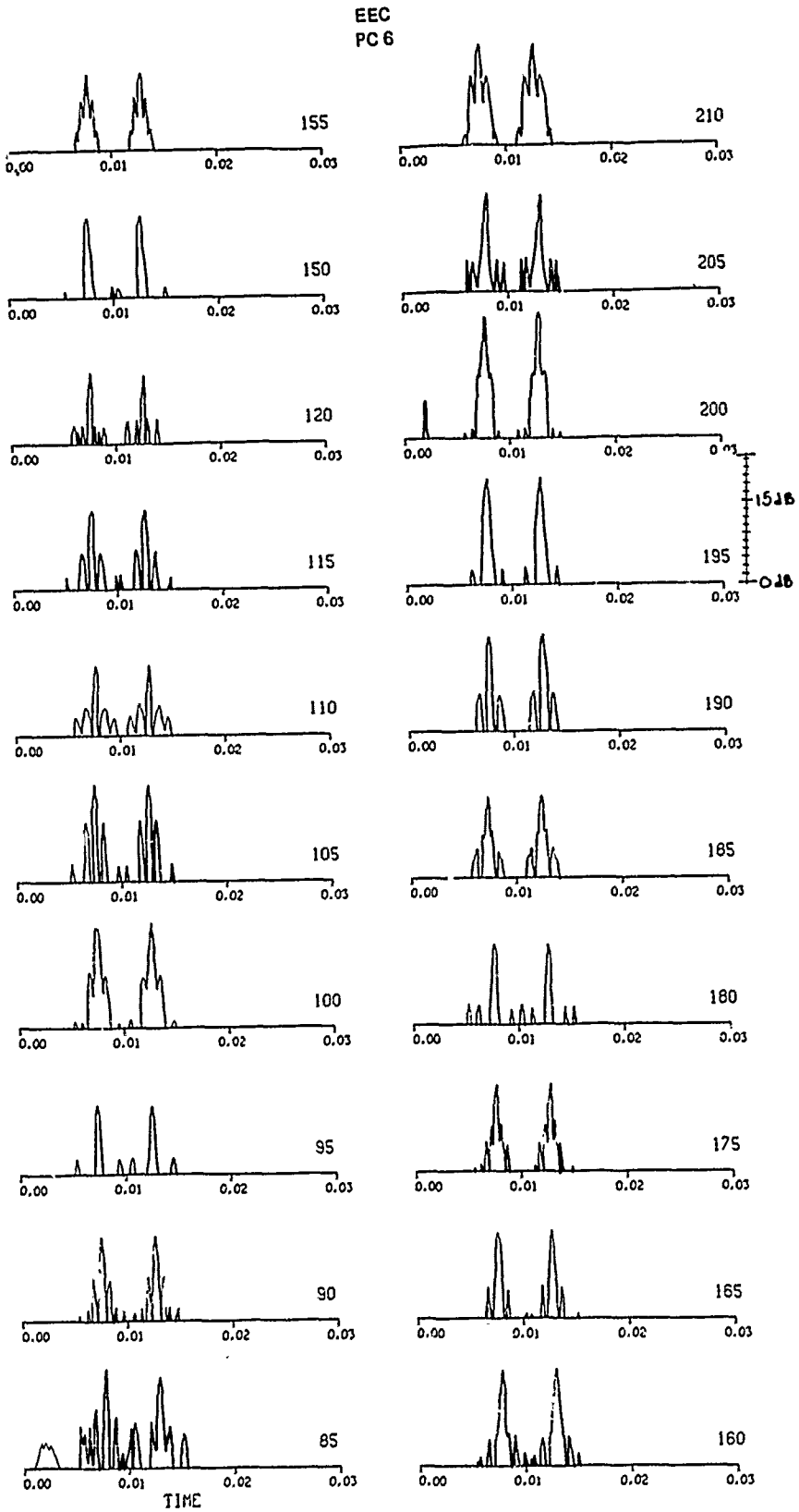

Figure 21. Pulse Code 6.

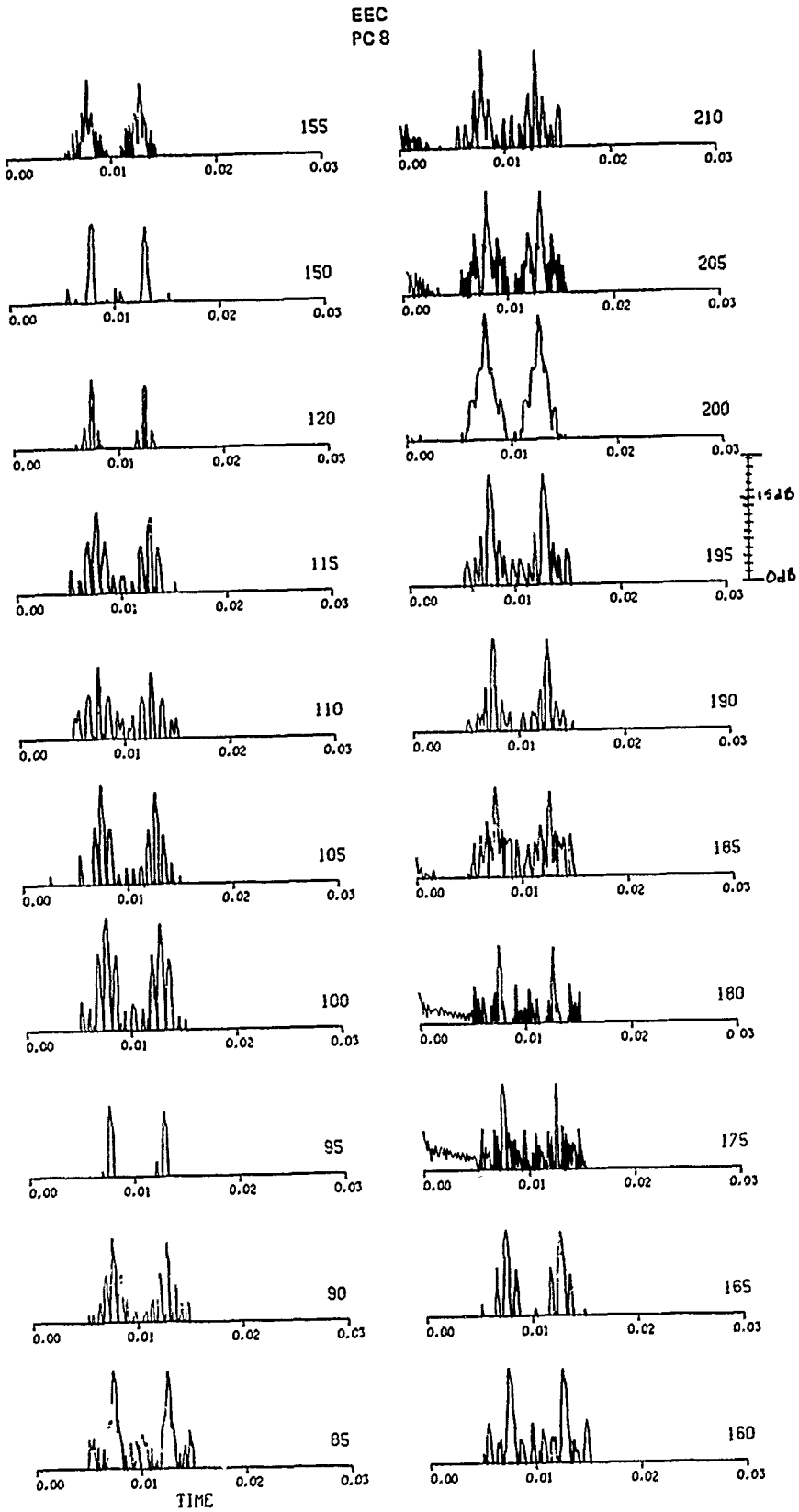

Figure 22. Pulse Code 8.

IV. RESULTS

The most striking feature of the echo plots (Figs. 3-10) is the extreme variability, both in echo shape and echo power. It should be recalled that the power in an echo was calculated as the mean square amplitude (prior to envelope detection). For the shapes shown here, it is likely that such a measure is not optimum, yet it remains a reasonable measure against which to compare later results. In an operational setting, however, computing the power in this way first requires that the echo be identified, and the echoes as shown might prove difficult to recognize in background interference. In such a case, some form of signal processing is needed to aid in echo identification.

The RC plots are shown in Figs. 11-19. Again one of the main features is the extreme variability in both shape and peak level. For an ideal echo, that is, one which matches the transmitted pulse, there would only be a single "spike" in the RC output when the echo had passed through the processor. A good example is shown in all RC plots at an aspect angle of 200 degrees (compare with the echo plots for the same angle). It is seen here that the transmitted pulse has essentially generated an echo from a single reflector on the target. In the case of PC4 (Figs. 6 and 14), the echo power is -27 dB and the RC peak is -28 dB, a very close agreement. At the other extreme, however, consider the results at an aspect angle of 110°. Again for PC4, the echo power is -38 dB, while the RC peak is -43 dB, a difference of 5 dB. For the higher resolution pulses, the differences tend to be somewhat greater.

It was anticipated that the higher resolution pulses would also tend to reveal more of the target structure than the smaller bandwidth pulses. In fact, this generally was not true. PC1 reveals very nearly as much structural detail as does PC3, except at aspect angles near 100°. It is thus concluded that for this target, spatial resolution less than 1 yard ($B \approx 1$ lHz) is not necessary when using RC processing. However, there may be a requirement for larger B to enhance the processing gain against reverberation.

The PRN echoes and RC curves (PC 7, 8) are quite disappointing in two respects. First, these echoes had a much poorer signal-to-noise ratio (not shown in the figures) than the other PC's, caused by the necessity of transmitting a reduced signal power in order to accommodate large signal amplitudes without distortion. Second, and perhaps because of the first effect, the RC plots are very ragged and lack the abrupt dropoff on either side of the main response lobe, as is demonstrated by the LFM RC curves. It would thus appear that this type of PRN pulse followed by RC would not be a suitable waveform in a noise-limited environment.

The EEC plots are shown in Figs. 19-22. A major difference between these and the RC curves is the single peak located precisely at the center of the EEC segment. Note also that the curves are symmetrical within a segment. Unlike the RC plots, which showed little increase in structural detail with increasing B, the EEC plots show definite improvement in this regard.

Of particular interest is the EEC result for the PRN pulses, PC 8 (Fig. 22). Compare this plot with the EEC result for PC 6 (Fig. 21) and with the RC result for PC 7 (Fig. 17). It is seen that the EEC process produces results which are very nearly identical for both LFM and PRN, and which are considerably more usable than RC for PRN pulses.

An analysis of Figs. 23-27 reveals that the loss between power and peak for RC increases with bandwidth, while the EEC values are relatively unaffected. This result is emphasized in Figs. 28 and 29, which show a comparison for RC and EEC, respectively, between an average (over PC) power level and the correlated peaks. On these figures, the loss shown at each aspect angle reflects that loss which occurred between power and peak for the same PC, as shown in the previous five figures. These results indicate that EEC is able to recombine the energy distributed throughout the echo, while RC is less able to do so.

The probe "echoes" were correlated with the stored replicas, and the results compared with the replica autocorrelations. No distortion or losses of any kind were discernible, which indicates that the transmit system did not distort the waveforms.

It was hypothesized that, in an ideal (Gaussian, white) noise background, any loss in the (average) correlated output would be due solely to target structural influences, even with a spatially stationary target. This was tested in the previously mentioned signal to noise analysis by using as the input power value the value of the respective peak (RC or EEC) shown in Figs. 23-27, rather than the power value shown there. It was found that the measured results then were in close agreement with the predicted values from Eq. (3) or (4), as appropriate. It is thus concluded that the hypothesis is correct, and that the theoretical processing capability of either RC or EEC is valid provided the input signal level can be determined.

Finally, it should be noted that Figs. 23-29 represent the target strength of this mine for the aspect angles indicated.* It must be emphasized that, in an operational environment, the raw echo could not be detected except at very high echo to interference levels, so that the sonar operator would have to rely on some form of echo processing to provide better detectability.

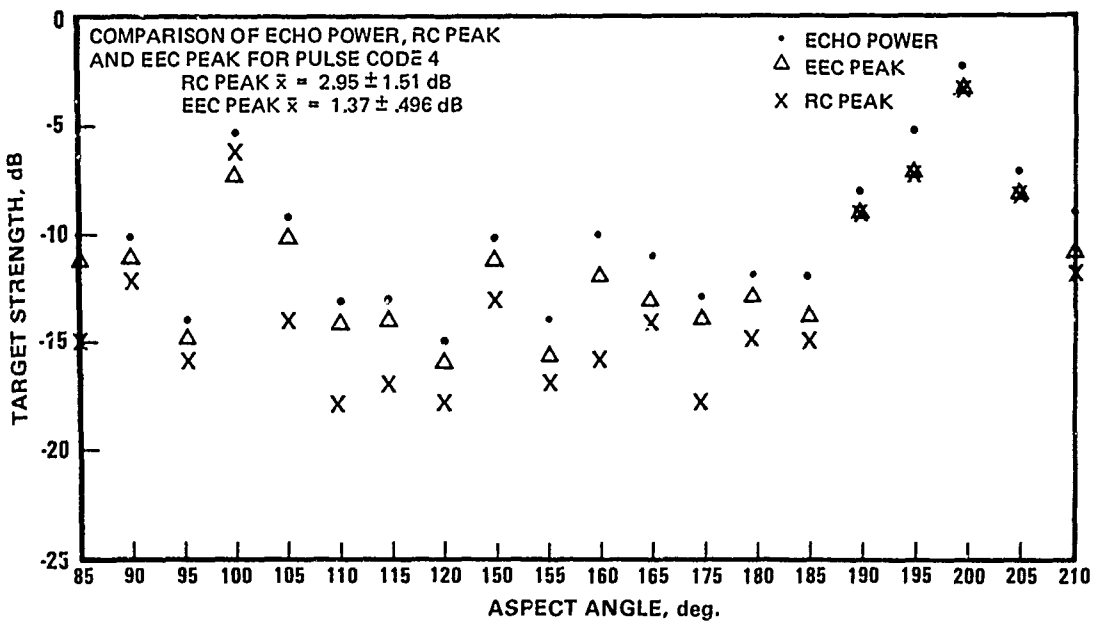

Figure 23. Comparison of Echo Power, RC Peak and EEC Peak for Pulse Code 4.

*based on calibrations supplied by ARL/UT.

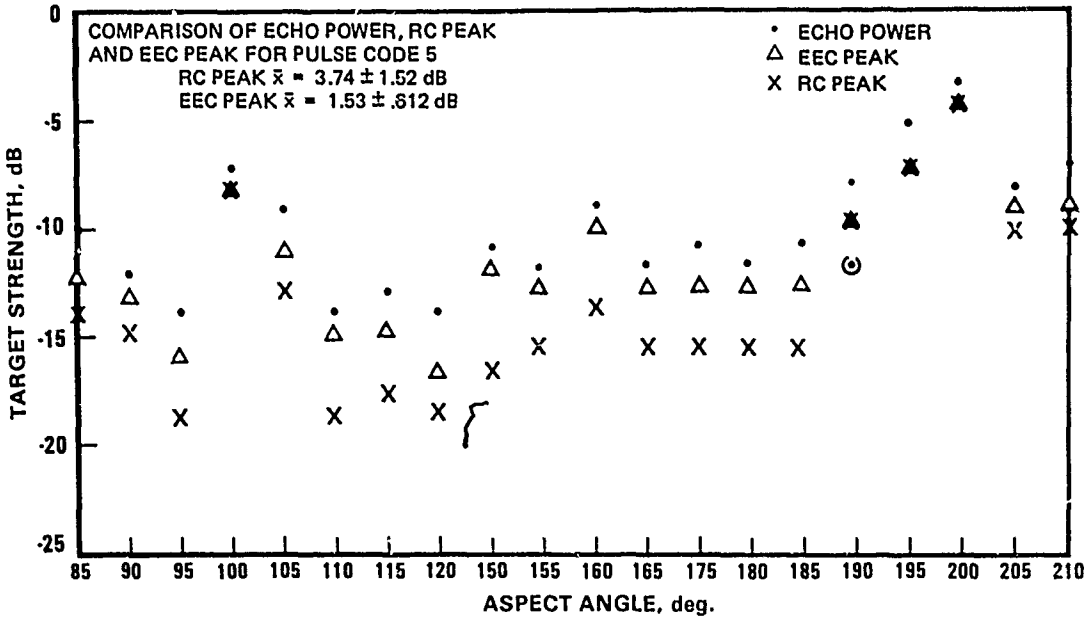

Figure 24. Comparison of Echo Power, RC Peak and EEC Peak for Pulse Code 5.

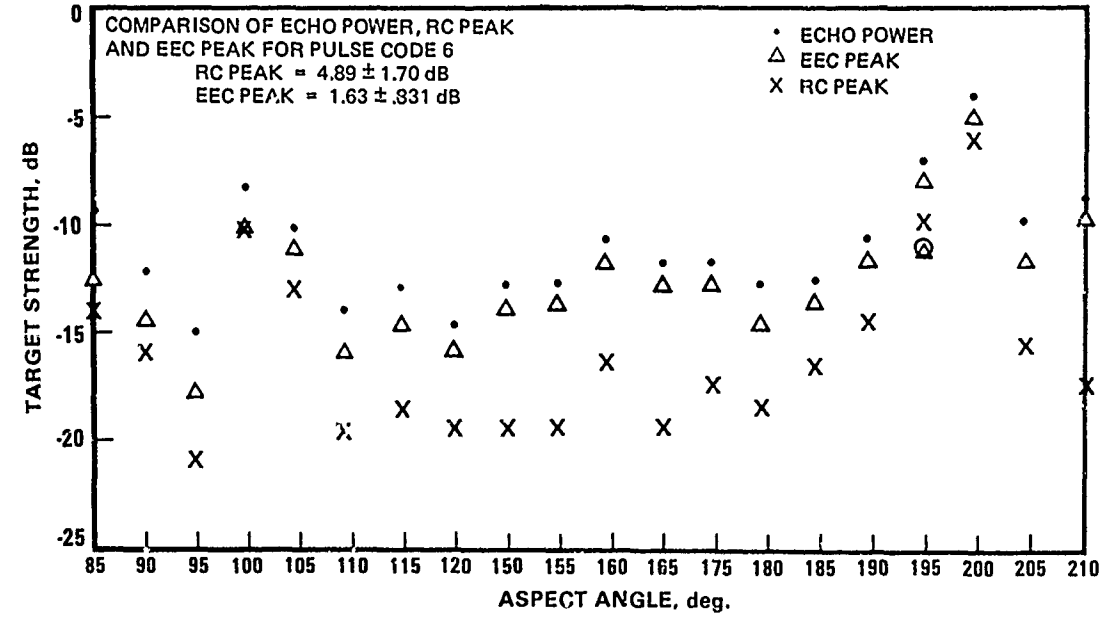

Figure 25. Comparison of Echo Power, RC Peak and EEC Peak for Pulse Code 6.

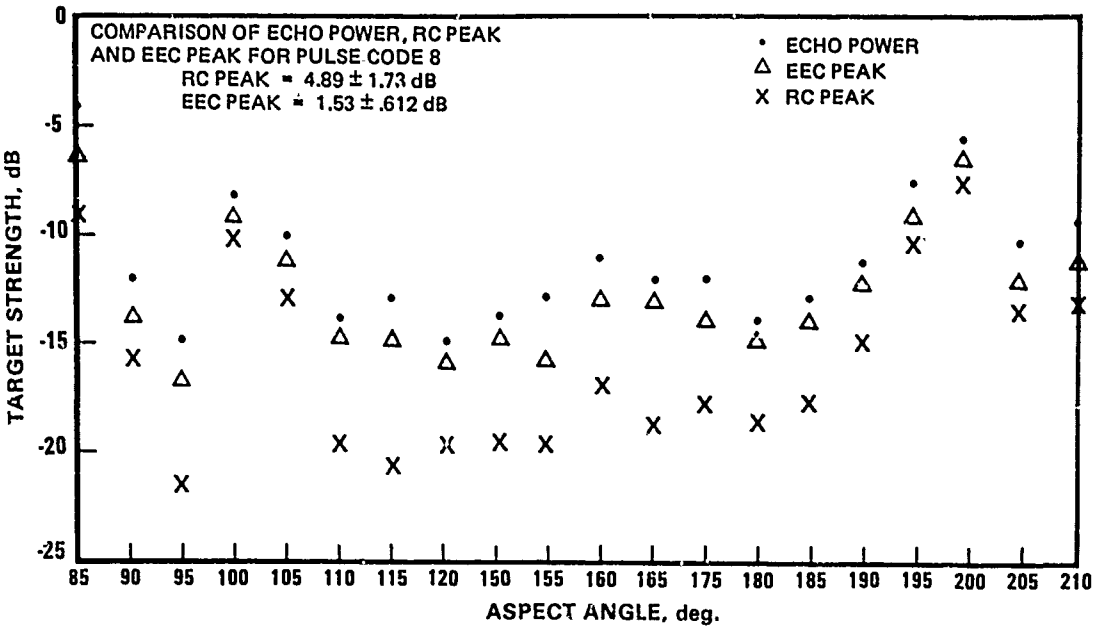

Figure 26. Comparison of Echo Power, RC Peak and EEC Peak for Pulse Code 8.

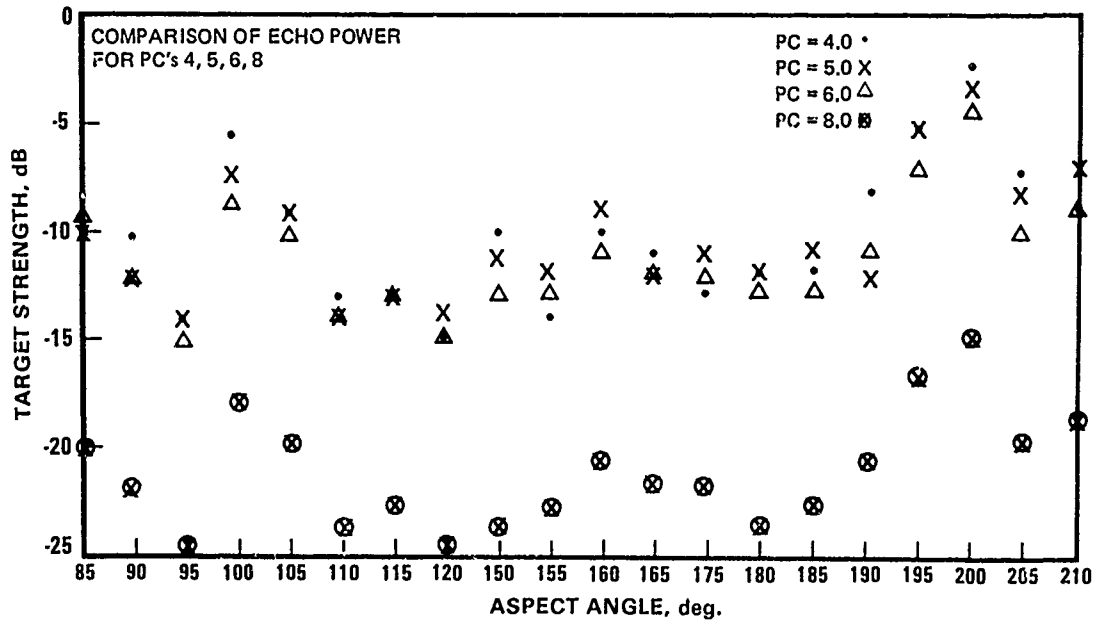

Figure 27. Comparison of Echo Power for PC's 4, 5, 6, 8.

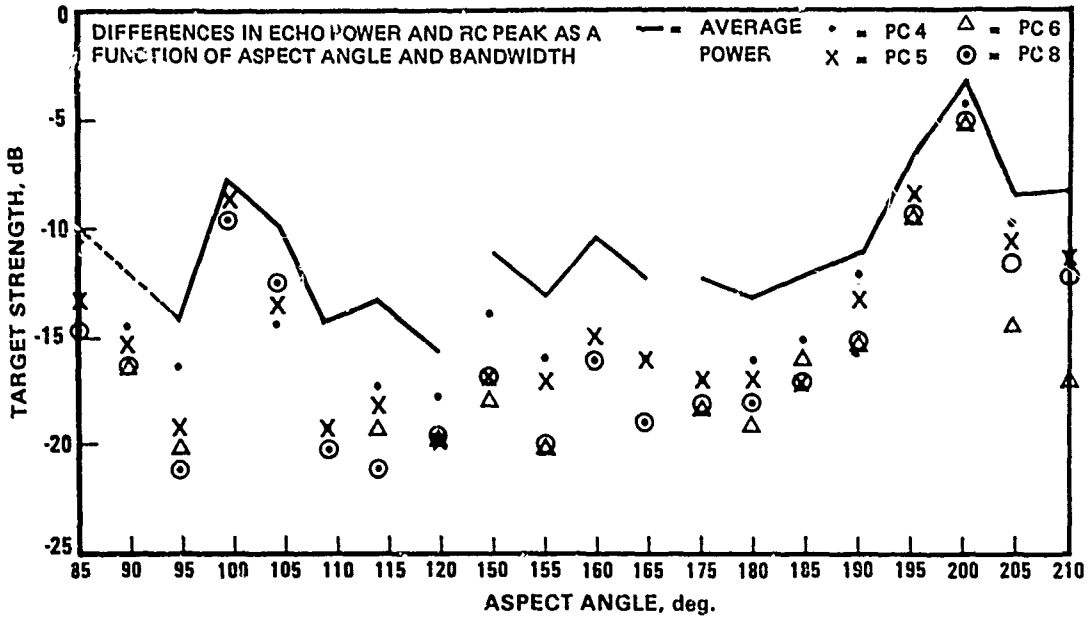

Figure 28. Differences in Echo Power and RC Peak as a function of aspect angle and bandwidth.

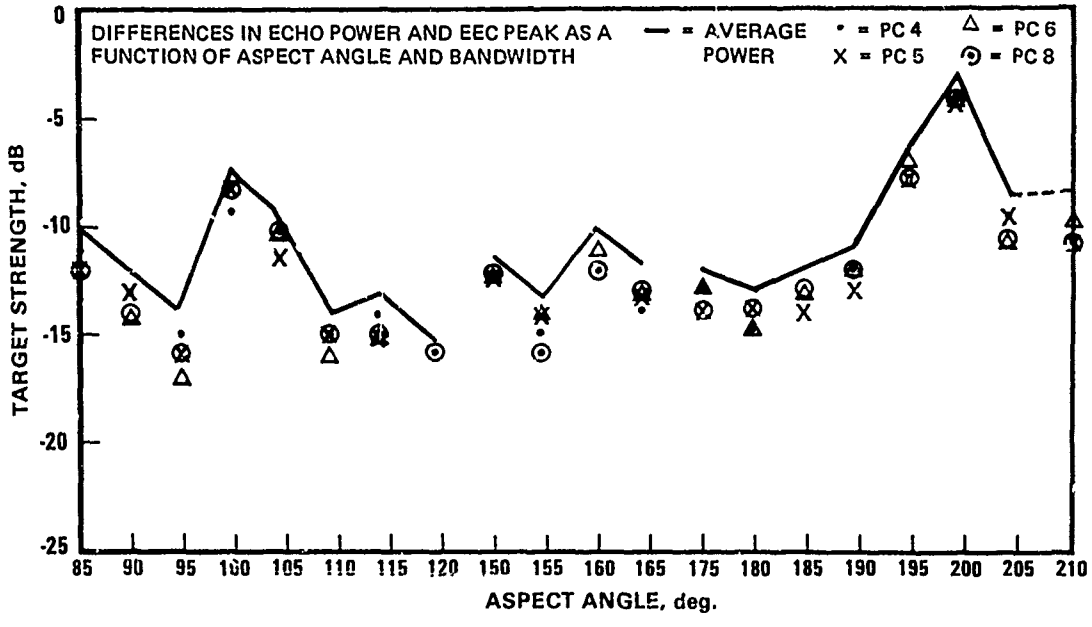

Figure 29. Differences in Echo Power and EEC Peak as a function of aspect angle and bandwidth.

V. DETECTION OF MINES

The purpose of this section is to discuss the detection of mines under an assumed scenario, and then relate the discussion to the results of the previous section.

Assume the following sonar requirements: resolution of 1 yard; pulse length τ = 75 ms for RC processing, τ = 25 ms for EEC processing; N = 20 beams in azimuth; own velocity uncertainty is ±1 kt; bearing uncertainty is ±1 beam. The false alarm problem is somewhat unusual and is as follows: there is a 50% probability of no false alarms in 1 hour. The observation time, T, is actually modified by limiting the attention of the observer to the last 2/3 of each ping history. Further, the decision rule will be based on two out of three occurrences, but this will be modified as indicated later.

The resolution capability requires a bandwidth of about B = 1 kHz. Thus $2B\tau = 50$ for EEC, and $2B\tau = 150$ for RC.

Figure 30 is an idealized plot of the probability density functions (pdf's) of the noise-only and signal-plus-noise distributions. The probability of false alarms is p′, so that p = 1 - p′. Now

prob [1 or more out of k events] =

1 – prob [zero out of k] =

$$1 - [(1-p')^k], \tag{5}$$

which is the binomial distribution for zero occurrences out of k trials. Define k to be

$$k = N \cdot B \cdot T \cdot 2/3 \tag{6}$$

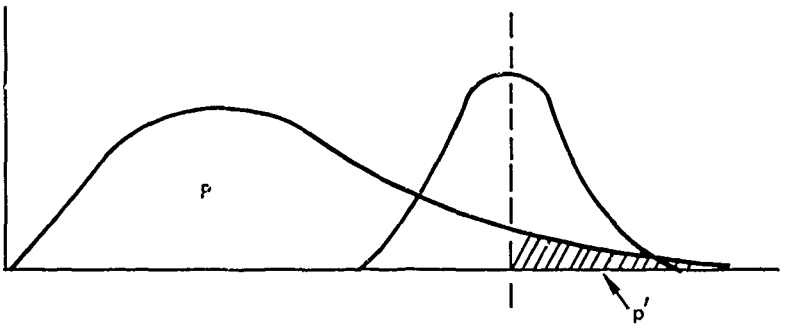

Figure 30. Idealized probability density functions.

The problem may be stated as follows: If there is a 50-percent probability of one or more false alarms in k trials, what is the required p′ of a single trial?

Thus

$$0.5 = 1 - [(1-p')^k] \tag{7}$$

or

$$p' = 1 - (0.5)^{1/k} \tag{8}$$

It is probable that the decision will not be made on a single threshold crossing, but rather on m crossings out of k possibilities. This again is a binomial distribution problem, as follows: The probability of m occurrences of an event in k independent trials is given by

$$P_{k;m} = \sum_{m} C_k^m \, p^m \, q^{k-m} \tag{9}$$

where

$$q = 1 - p$$

$$C_k^m = \frac{k!}{m!\,(k-m)!}$$

Assuming two out of three trials defines the decision rule,

$$P_{k;m} = \frac{3!}{2!\,(3-2)!}\,(\bar{p}')^2\,(q') + \frac{3!}{3!\,(3-3)!}\,(\bar{p}')^3$$

$$\simeq 3(\bar{p}')^2$$

$$= p' \text{ (Eq. (8)).} \tag{10}$$

where $\bar{p}'$ is the required probability of false alarms for one event necessary to meet the decision rule.

The rate of exceeding a threshold is the False Alarm Rate, K. When B is large an approximation is (Ref. 7)

$$K' = \bar{p}'\,B. \tag{11}$$

Assuming that the operator is observing the detected envelope of the correlation, one may use the following: define the recognition differential to be (Ref. 5)

$$d = 20 \log [(D - \sigma\sqrt{\pi/2})/0.655\sigma]$$

$$D = [-2\sigma^2 \ell n(K'/B)]^{1/2}$$

(B in Hz)
(assume $\sigma = 1$). (12)

Using curves from Ref. 5, one obtains from d the 50% Signal Differential (SD) or signal-to-noise ratio (in dB) into the correlator necessary to achieve the probability of false alarms, $\bar{p}'$, for a 50% probability of detection. However, for EEC, it is possible to reduce K' simply by not computing the correlations except about the zero lag position. The minimum K for EEC is about $K'/2B\tau$. When the target or own ship has a velocity uncertainty, that uncertainty will define the minimum K for EEC. For the stated uncertainty of v = 1 kt, one has

$$\Delta R = v\tau = 1.68 \text{ ft/sec} \cdot 0.025 \text{ sec} = 4.2 \times 10^{-2} \text{ ft} \quad (13)$$

so that

$$\delta = \Delta R/C = 8.4 \times 10^{-6} \text{ sec.}$$

EEC compensates for this time uncertainty merely by searching the correlation output for $\pm\delta$ seconds about the zero lag position. The maximum reduction in the output duration compared with the input duration is

$$\alpha = 2\delta/\tau,$$

however, for security, let us search 5δ, so that

$$\alpha = 1.68 \times 10^{-3}. \quad (14)$$

Then for EEC

$$\hat{K} = K'/\alpha. \quad (15)$$

Using the above-mentioned curves, one has for RC

$$SD = -9.8 \text{ dB} \quad (16)$$

while for EEC

$$SD = -5.3 \text{ dB} \quad (17)$$

At this point, one must more carefully account for the uncertainty in own ship's velocity. The assumption of ±1 knot potential error, combined with an illumination of a given sea volume every 10 seconds, causes a potential range uncertainty of ±6 yards. Replica correlation provides a much more precise estimate of target range than does EEC, and is correspondingly more sensitive to uncertainties in velocity. Since ±6 yards is approximately equal to ±6 resolution cells, the following rule is assumed for RC: Whenever the output from any one resolution cell exceeds a threshold in one transmission, the next transmission will require the observer to consider 6 resolution cells on either side of the original cell as potentially containing the echo from the same original target. On the third transmission, the observer will then be required to observe a total of 25 cells. The situation is further compounded by the beam uncertainty. Again for RC, the 3-beam rule requires that 39 cells be searched on the second transmission, while 125 cells are searched on the third. See figure 31. For EEC, on the other hand, the inherent range uncertainty is $c\tau = \pm 41$ yards, so that the velocity uncertainty is transparent to an observer at a fixed range. However, two transmissions will result in a compounded potential error of ±12 yards, which is 29% of the inherent uncertainty. Thus it will be assumed that, for EEC, the following rule applies: When an echo is identified on one transmission, the second transmission will necessitate the observation of 3 cells (1 range cell by 3 beam cells), while the third transmission will require the observation of a total of 10 cells.

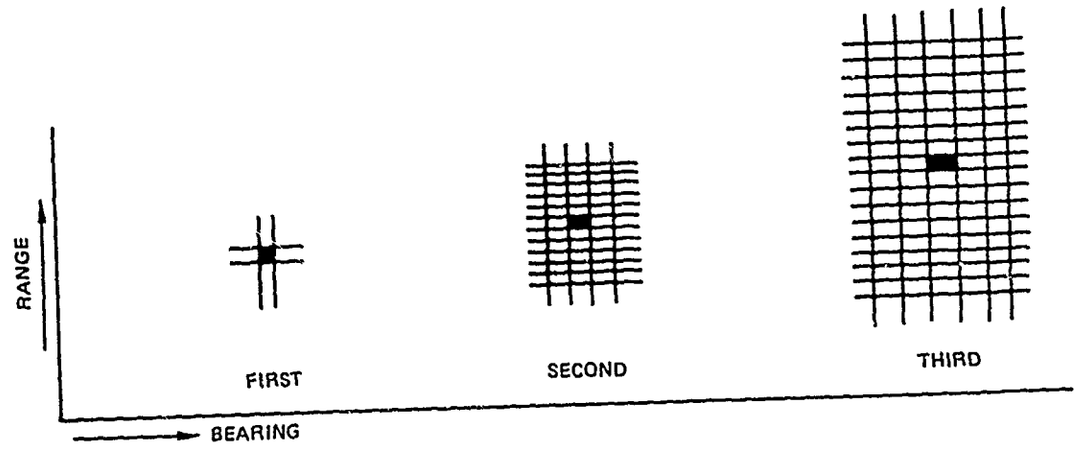

Figure 31. Multiping range and bearing uncertainty.

The probabilities previously calculated did not include the velocity uncertainties. Thus, restating the problem: Given a probability $\hat{p}$ of a single occurrence on the first ping, what is the probability of an occurrence in the second ping or in the third ping? It should be noted that an occurrence on the first ping presupposes a single target, so that the probability of more than one cell being "occupied" on the second or third ping is very small. From Eq. (9), for RC,

$$P_{39;1} = 39 \cdot \hat{p}(1-\hat{p})^{38}$$

$$\simeq 39\,\hat{p}(1-38\hat{p})$$

(For the second ping) (18)

and

$$P_{125;1} = 125 \cdot \hat{p}(1-\hat{p})^{124}$$

$$\simeq 125 \cdot \hat{p}(1-124\hat{p})$$

(For the second ping) (19)

So, for RC, the total probability, which is equal to p' [Eq. (8)], is

$$p' = \hat{p} \cdot p_{39;1} + \hat{p} \cdot p_{125;0} \cdot p_{125;1}$$

$$\simeq 39\hat{p}^2 + 125\hat{p}^2$$

$$= 164\hat{p}^2 . \quad (20)$$

For EEC, we have

$$p_{3;1} = 3 \cdot \hat{p}(1-\hat{p})^2$$

$$\simeq 3\hat{p}$$

(For the second ping) (21)

and

$$p_{10;1} \simeq 10 \cdot \hat{p}$$

(For the third ping) (22)

Thus the total probability for EEC is

$$p' = 3\hat{p}^2 + 10\hat{p}^2$$

$$= 13\hat{p}^2. \quad (23)$$

The results may finally be given as in Table 2.

	$\hat{p}$	(K'/α)	d	SD
RC	9.37×10^{-6}	9.37×10^{-3}	14.7	-8.7
EEC	3.33×10^{-5}	19.82	7.5	-4.5

(Note: $\alpha = 1.0$ for RC)

Table 2. Signal differentials.

These results indicate that EEC requires approximately 4 dB greater SNi than does RC, for a perfect, matched echo. However, from Fig. 23, it is seen that RC, on the average, suffers 3 ± 1.5 dB "splitting" loss for PC 4, whereas EEC suffers an average reduction in power recombination of 1.4 ± 0.5 dB. However, the maximum EEC loss for this pulse code was 2 dB, whereas that for RC was 5 dB. In addition, the difficulty in displaying 27,000 output samples to the operator will probably require a reduction in the number of points through "peak picking" or "or-ing" (Ref 8). Such a reduction, for the recognition differential (d) listed in Table 2, will entail an additional loss in S.D. for RC of at least several dB. This would place the SD for RC about equal to that required for EEC.

VI. DISCUSSION

CORRELATION

For a given pulse bandwidth, EEC requires three times the pulse length necessary for RC for a given BT product. For systems which require short transmit times, either for electronic or security reasons, this may be a serious difficulty. EEC does not provide precise range information as does RC. There is an ambiguity in the range comparable to the travel time of one third of the transmitted triplet pulse. However, the resolution capability of EEC is the same as for RC. EEC has the following advantages over RC:

1. Simplicity of Processing. Replica correlation, even when done by "fast correlation," is a time consuming, and/or hardware consuming operation. The array processor necessary to satisfy system requirements is likely to be large and expensive. EEC, on the other hand, may be accomplished by simple time-domain correlation in real-time, since only those correlation lags necessary to account for unknown Doppler must be computed.

2. Reduced Display Requirements. It is estimated that, using a 1-kHz B pulse in an operational setting, RC processing will require the observation of 27,000 spatial resolution cells per transmission for 20 beams. EEC will require the observation of only 900 such cells.

3. Energy Recombination. The structural properties of the target will produce a "split" echo. RC is not capable of recombining this energy, whereas EEC does so very well. In addition, RC shows increased decorrelation with increasing bandwidth, whereas EEC does not seem to be so affected.

4. False Alarm Rate. The false alarm rate for EEC may be greatly reduced simply by not computing the correlation function at times far removed from the zero lag (segment center). This has the effect of reducing required detection thresholds, thus improving target detectability.

5. Target Motion. For the waveforms studied here, RC processing is extremely sensitive to target and/or own-ship velocity, and may show severe distortion in the presence of uncorrected accelerations. A more appropriate waveform to use in such a case is linear period modulation (LPM), which, for RC, will provide Doppler tolerance. However, accelerations will still prove highly distorting. For EEC, using LPM pulses, the results will be insensitive to Doppler, and highly tolerant of constant or slowly varying accelerations.

6. Pseudorandom Noise. It appears that PRN pulses of the type used here will not be appropriate for RC processing in a noise environment, but will, aside from the reduced transmit power mentioned previously, work as well as LFM pulses for EEC processing.

TARGET STRENGTH

With high-resolution pulses, the concept of target strength is somewhat ambiguous. One must discuss this measure in terms of the signal processing to be used, and it must be clear if the measure is an average over some spatial extent of the echo or is a peak value. Assuming that coherent echo processing is operationally required, the processor must decide whether to average the correlation output over some time greater than the basic resolution of the pulse, or not. It is the author's contention that a proper averaging time is totally

dependent on the aspect angle of the target, and that, without such information, post-correlation averaging will be counterproductive. However, any post correlator/detector averaging suitable for RC would be identically suitable for EEC, so the comparison of the two is valid, independent of this additional processing. The results presented here reflect that which a sonar operator would encounter, provided the background interference is a noise limiting environment. However, for large bandwidth signals, it is felt that the same results will apply for a reverberation interference.

VII. CONCLUSIONS

An investigation of the acoustic response of a particular mine has been presented in terms of aspect angle dependency and signal processing. It has been demonstrated that EEC is superior to RC for recombining "split" energy from this mine and the results indicate that EEC would be operationally superior to RC in mine detection in a noise-limited environment.

In addition to investigating this one target, it has been demonstrated that an effective, rapid methodology is available for obtaining the acoustic signature of any small mine or torpedo-like object for any pulse type conceivable. Signal processing techniques such as simple averaging, RC, and EEC are available, and others can be incorporated.

VIII. RECOMMENDATIONS

A similar series of tests should be conducted in reverberation environments to determine the relative effect on RC and EEC.

IX. REFERENCES

1. C. W. Helstrom, Statistical Theory of Signal Detection, Pergamon Press Ltd, New York, 1968.

2. J. S. Bendat, A. G. Piersol, Random Data: Analysis and Measurement Procedures, Wiles Interscience, New York, 1971.

3. Available to those with need to know.

4. M. D. Green, "Replica Correlation of Linear Period Modulated (LPM) Signals," NOSC TR 228, June 1978.

5. M. D. Green, "Echo-Echo Correlation," NOSC TR 336, August 1979

6. Applied Research Laboratory, University of Texas, Austin, Texas, "Target Strength Measurement Facility," by B. F. Tupa, Sept 1979.

7. P.B. Brown, "A Comparison of the Performance of Several Signal Processors," TRACOR no. 66-203-U, March 10, 1966.

8. M.B. Montgomery, "Final Technical Report on Task 2, NO bsr - 95149 Mod 9 AN/SQS - 26 Display Analysis." TRACOR Document no. 68-633-U, 1 June 1968.

X. APPENDIX: ECHO-ECHO CORRELATION

The purpose of this appendix is to provide a brief summary of the EEC technique. For more detailed information, the reader is directed to Ref. 5.

Consider the envelope of an acoustic transmission such as is shown in Fig. A1. Note that the individual length, τ, of each pulse in the triplet is $\leqslant$ L. Assume that the range of the target is unknown. Immediately upon completion of the transmission (at time 3L). begin partitioning the received time history (RTH) into segments, each L seconds in length. After some time commensurate with the range of the target, an echo set such as shown in figure A2 will be received. Note the arbitrary alignment of the echoes vis-a-vis the segmentation. At any time prior to the arrival of the echo set, take segment X_K, sample it and correlate it with the sampled version of segment X_{K+1}, as indicated in Eq. (A1).

$$C_K(\lambda) = \frac{1}{2L} \sum_{j=-L}^{+L} X_K(j+\lambda)\, X_{K+1}(j) . \qquad \text{(A1)}$$

Next, discard segment X_K and correlate X_{K+1} with X_{K+2}, obtaining $C_{K+1}(\lambda)$. Note that if segments X_K and X_{K+1} both contain only noise, then the expected value of $C_K(\lambda)$ is zero. The same is true if X_{K+1} is noise only, while X_{K+2} is signal plus noise. However, if X_{K+2} and X_{K+3} both contain echo, then the expected value of $C_{K+2}(\lambda)$ is the autocorrelation of the echo, contaminated with noise.

An inspection of this process reveals two important items:

1. For a spatially stationary target, the peak of the echo correlation falls precisely at $C_{K+2}(0)$, ie, at the center of the segment.

2. Based on item 1, above, it is only necessary to compute $C_{K+2}(\lambda)$ at $\lambda = 0$, unless the target is moving. In this case, one need compute $C_{K+2}(\lambda)$ only for values of $\delta \leqslant |\lambda\text{max}| = V\tau/c$, where V = target velocity (relative), C = sonic speed. Thus the opportunity for a false alarm is reduced in relation to V.

The EEC plots shown in the text represent $|\lambda\text{max}| = 2.5$ ms. While each time mark on the abscissa represents 25 ms of elapsed time, the resolution between time marks is only 5 ms. Thus, while the actual elapsed time to the target is known only to within 25 ms, the basic resolution of the pulse is retained, and is the same as for RC.

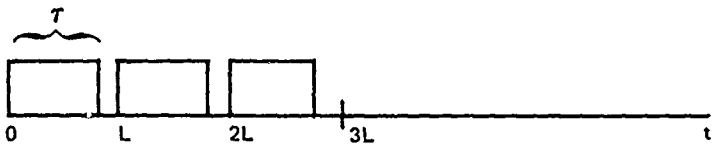

Figure A1. EEC ping sequence.

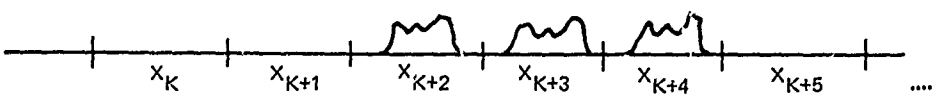

Figure A2. EEC echo sequence.